Gas-phase products and secondary aerosol yields from the photooxidation of 16 different terpenes

Anita Lee,[1] Allen H. Goldstein,[1] Jesse H. Kroll,[2] Nga L. Ng,[2]
Varuntida Varutbangkul,[2] Richard C. Flagan,[2] and John H. Seinfeld[2]

Received 4 January 2006; revised 18 April 2006; accepted 16 May 2006; published 7 September 2006.

[1] The photooxidation of isoprene, eight monoterpenes, three oxygenated monoterpenes, and four sesquiterpenes were conducted individually at the Caltech Indoor Chamber Facility under atmospherically relevant HC:NO_x ratios to monitor the time evolution and yields of SOA and gas-phase oxidation products using PTR-MS. Several oxidation products were calibrated in the PTR-MS, including formaldehyde, acetaldehyde, formic acid, acetone, acetic acid, nopinone, methacrolein + methyl vinyl ketone; other oxidation products were inferred from known fragmentation patterns, such as pinonaldehyde; and other products were identified according to their mass to charge (m/z) ratio. Numerous unidentified products were formed, and the evolution of first- and second-generation products was clearly observed. SOA yields from the different terpenes ranged from 1 to 68%, and the total gas- plus particle-phase products accounted for ~50–100% of the reacted carbon. The carbon mass balance was poorest for the sesquiterpenes, suggesting that the observed products were underestimated or that additional products were formed but not detected by PTR-MS. Several second-generation products from isoprene photooxidation, including m/z 113, and ions corresponding to glycolaldehyde, hydroxyacetone, methylglyoxal, and hydroxycarbonyls, were detected. The detailed time series and relative yields of identified and unidentified products aid in elucidating reaction pathways and structures for the unidentified products. Many of the unidentified products from these experiments were also observed within and above the canopy of a Ponderosa pine plantation, confirming that many products of terpene oxidation can be detected in ambient air using PTR-MS, and are indicative of concurrent SOA formation.

Citation: Lee, A., A. H. Goldstein, J. H. Kroll, N. L. Ng, V. Varutbangkul, R. C. Flagan, and J. H. Seinfeld (2006), Gas-phase products and secondary aerosol yields from the photooxidation of 16 different terpenes, *J. Geophys. Res.*, *111*, D17305, doi:10.1029/2006JD007050.

1. Introduction

[2] Biogenic emissions of terpene compounds influence atmospheric chemistry through the formation of tropospheric ozone (O_3) and the production of secondary organic aerosol (SOA). Terpenoids (or isoprenoids) encompass several wide classes of compounds, including hemiterpenes (isoprene, C_5H_8), monoterpenes ($C_{10}H_{16}$), sesquiterpenes ($C_{15}H_{24}$), and oxygenated terpenes (e.g. $C_{10}H_{18}O$, $C_{10}H_{12}O$). Terpenoids are emitted from deciduous and evergreen trees as a function of temperature, or of both temperature and light [*Kesselmeier and Staudt*, 1999]. Terpenes, with their unsaturated carbon bonds, are reactive with OH, O_3, and NO_3, the common atmospheric oxidants, with lifetimes that range from minutes to hours [*Atkinson and Arey*, 2003]. Several monoterpene oxidation products are known to undergo gas-particle partitioning, including nopinone, pinonaldehyde, pinic acid, and pinonic acid, and have been observed in ambient air in the gas and particle phases [*Yu et al.*, 1999; *Kavouras et al.*, 1999].

[3] Experiments examining terpene oxidation have been conducted since F. W. Went first suggested the blue haze in forested regions were products of these reactions. Early experiments determined rate constants for the reaction of many different terpenes with the major atmospheric oxidants [e.g., *Atkinson et al.*, 1989; *Shu and Atkinson*, 1994], and yields of SOA [e.g., *Pandis et al.*, 1991; *Hoffmann et al.*, 1997]. Experiments also examined gas-phase products from the oxidation of isoprene [*Tuazon and Atkinson*, 1990] and common monoterpene species, such as α- and β-pinene [*Grosjean et al.*, 1992; *Arey et al.*, 1990; *Hakola et al.*, 1994], as well as a broader suite of monoterpenes [*Shu et al.*, 1997; *Reissell et al.*, 1999; *Orlando et al.*, 2000]. SOA yield from isoprene has been long thought to be negligible [*Pandis et al.*, 1991]. However, recent observations of tetrol

[1]Department of Environmental Science, Policy, and Management, University of California, Berkeley, Berkeley, California, USA.
[2]Department of Environmental Science and Engineering and Department of Chemical Engineering, California Institute of Technology, Pasadena, California, USA.

0148-0227/06/2006JD007050

compounds with an isoprene skeleton [*Claeys et al.*, 2004; *Kourtchev et al.*, 2005] and isoprene oxidation products [*Matsunaga et al.*, 2005] in ambient aerosol suggest that isoprene does contribute to ambient SOA production. Additionally, the high global isoprene emission rate (500 Tg $year^{-1}$) [*Guenther et al.*, 1995] and the 1–3% SOA yield obtained from the photooxidation of isoprene at lower temperatures and initial isoprene concentrations [*Kroll et al.*, 2005], also suggest that isoprene oxidation may represent an important contribution to global SOA production.

[4] The HC:NO_x ratio has been shown to impact SOA production. *Pandis et al.* [1991] showed that increasing the HC:NO_x ratio increased SOA yield when the ratio was $<\sim$10–15 ppb HC: ppb NO_x, but decreased SOA yield at higher ratios. From isoprene photooxidation under high NO_x, SOA yield decreased with increasing NO_x [*Kroll et al.*, 2006]. Experiments with HC:NO_x ratios >8 were reported to increase SOA production from *m*-xylene [*Song et al.*, 2005]. Additionally, higher NO_x levels in the chamber increase O_3 formation, which may impact SOA yield due to possible O_3 reactions. Low HC:NO_x ratios ($\sim$3–6 ppb HC: ppb NO_x) are generally representative of ambient air observed above Blodgett Forest, a Ponderosa pine plantation in the Sierra Nevada, California, where typical NO_x concentrations are $\sim$1–2 ppb [*Day et al.*, 2002] and the sum of mixing ratios of all typically measured biogenic and anthropogenic VOCs in ambient air, that have a lifetime on the order of the time scale of these experiments, is $\sim$5–6 ppb [*Lamanna and Goldstein*, 1999]. Thus, chamber experiments conducted at low HC:NO_x ratios (i.e., high NO_x) may be more applicable to the real atmosphere in forested environments.

[5] Recent studies provide observational support that terpenes can be oxidized within a forest canopy before detection by above-canopy flux techniques. In an orange grove in Spain, β-caryophyllene, a reactive sesquiterpene, was observed in branch enclosures but not in simultaneous measurements above the canopy, suggesting that β-caryophyllene was oxidized within the canopy [*Ciccioli et al.*, 1999]. At Blodgett Forest, chemical O_3 flux to the ecosystem scaled exponentially with temperature in a similar manner as monoterpenes [*Kurpius and Goldstein*, 2003], and from the same site, elevated monoterpene fluxes to the atmosphere from the mastication of Ponderosa pine trees [*Schade and Goldstein*, 2003] resulted in increased chemical O_3 flux to the ecosystem [*Goldstein et al.*, 2004], suggesting a linkage between chemical O_3 loss in the canopy and terpene emissions. In subsequent work, *Holzinger et al.* [2005] observed large quantities of previously unmeasured oxidation products above the same pine forest canopy. In a northern Michigan forest, elevated nighttime OH concentrations correlated with O_3 mixing ratios, suggesting that OH was produced from reactions between O_3 and unmeasured terpenes [*Faloona et al.*, 2001]. From the same forest, higher than expected OH reactivity was observed and scaled exponentially with temperature in a similar manner as biogenic emissions [*Di Carlo et al.*, 2004]. Taken together, these results provide convincing evidence of chemical loss of reactive compounds within the forest canopy through oxidation by OH and O_3.

[6] Previously, we reported the yields of SOA and gas-phase products from the ozonolysis of ten terpene compounds [*Lee et al.*, 2006]. Here, we report the results from a series of chamber photooxidation experiments conducted on 16 terpene compounds in the presence of OH, NO_x, hυ, and secondarily-produced O_3. Yields of SOA and gas-phase products are presented, as well as the time evolution of selected calibrated gas-phase oxidation products, and gas-phase oxidation products identified by their mass to charge ratio (*m*/*z*). A more detailed analysis of the contribution of first and second-generation oxidation products to SOA production is presented elsewhere [*Ng et al.*, 2006]. The goal of the PTR-MS measurements of gas-phase oxidation products from the ozonolysis and photooxidation of terpenes is to confirm if ions observed at Blodgett Forest are consistent with terpene oxidation, and to provide a guide to future studies using PTR-MS to monitor secondary gas-phase compounds in ambient air. Here, we present the yields of the observed oxidation product ions, and focus on the two product ions that were dominant at Blodgett Forest, *m*/*z* 113 and 111.

2. Experiment

[7] The photooxidation experiments were conducted at the Caltech Indoor Chamber Facility, which has been described in detail elsewhere [*Cocker et al.*, 2001; *Keywood et al.*, 2004]. Briefly, the facility consists of two suspended 28 m^3 flexible Teflon chambers that maintain atmospheric pressure at all times. For the monoterpene, isoprene, and oxygenated terpene experiments, ammonium sulfate seed aerosol was added to act as a surface for the condensation of oxidation products, contributing to the measured yield of secondary organic aerosol. For the sesquiterpene experiments, no initial seed aerosol was used because nucleation from sesquiterpene oxidation would result in two aerosol modes, making data analysis, particularly the wall loss correction, difficult. The starting concentration of seed aerosol was about 20,000 particles cm^{-3}, with a mean diameter of 80–100 nm. SOA yields were calculated from each experiment from the ratio of the amount of SOA formed (assuming density of 1.25 g cm^{-3}) and the amount of hydrocarbon reacted. The hydrocarbon to NO_x ratio (HC:NO_x) for all experiments ranged from 0.7–2.2 ppb HC: ppb NO_x. O_3, produced from the photolysis of NO_2 inside the chamber, was measured using an ambient O_3 monitor (Horiba APOA-360, Irvine, CA), and calibrated using an internal O_3 generator and N_2 as zero air.

[8] Microliter volumes of individual liquid monoterpenes and oxygenated terpenes were injected into a 250 mL glass bulb and gently heated as a stream of clean air passed through the bulb, vaporizing the terpene and carrying it into the chamber. The radical precursor used was nitrous acid (HONO), prepared by dropwise addition of 2 mL of 1% $NaNO_2$ into 15 mL of 10% H_2SO_4 in a glass bulb attached to the chamber. A stream of dry air was passed through the bulb, introducing HONO into the chamber. A NO_x monitor (Horiba APNA-360, Irvine, CA) measured NO and NO_2, which were formed as side products in the preparation of HONO. HONO was detected by the PTR-MS at *m*/*z* 30, the dehydrated fragment of $HONOH^+$, but not at the parent ion *m*/*z* 48, and also appeared to be detected by the NO_x monitor. However, HONO calibrations were not per-

Table 1. Parent Terpene Compounds, Listed in Order of Decreasing Aerosol Yield

Compound	Structure	Formula (m/z)	k_{OH},[a] cm^3 $molec^{-1}$ s^{-1}	Compound	Structure	Formula (m/z)	k_{OH},[a] cm^3 $molec^{-1}$ s^{-1}
β-caryophyllene		$C_{15}H_{24}$ (205)	2.0×10^{-10}	α-pinene		$C_{10}H_{16}$ (137)	5.3×10^{-11}
α-humulene		$C_{15}H_{24}$ (205)	3.0×10^{-10}	terpinolene		$C_{10}H_{16}$ (137)	2.3×10^{-10}
longifolene		$C_{15}H_{24}$ (205)	4.8×10^{-11}	β-pinene		$C_{10}H_{16}$ (137)	7.7×10^{-11}
limonene		$C_{10}H_{16}$ (137)	1.7×10^{-10}	γ-terpinene		$C_{10}H_{16}$ (137)	1.8×10^{-10}
myrcene		$C_{10}H_{16}$ (137)	2.1×10^{-10}	α-terpinene		$C_{10}H_{16}$ (137)	3.6×10^{-10}
methyl chavicol		$C_{10}H_{12}O$ (149)		verbenone		$C_{10}H_{14}O$ (151)	
3-carene		$C_{10}H_{16}$ (137)	8.7×10^{-11}	linalool		$C_{10}H_{18}O$ (155)	1.6×10^{-10}
aromadendrene		$C_{15}H_{24}$ (205)		isoprene		C_5H_8 (69)	9.9×10^{-11}

[a]Rate constants were obtained from *Atkinson and Arey* [2003, and references therein].

formed, so its concentration in the chamber was not well-constrained.

[9] When the seed, parent hydrocarbon, and NO_x concentrations stabilized, turning on the blacklights started the reactions. The indoor chambers were equipped with 276 GE350BL fluorescent blacklights centered at 354 nm, efficiently photolyzing HONO to OH and NO. To minimize temperature increases (1–2°C over the course of the experiment), 10% of the lights were used. Between experiments, the chambers were continuously flushed with clean compressed air that passed through four scrubbing cartridges containing activated carbon, silica gel, Purafil, and molecular sieve, respectively, and a HEPA filter before entering the Teflon chambers. The chambers were flushed for at least 36 h before the start of an experiment, which reduced O_3 and particle concentrations to below 1 ppb and 100 particles cm^{-3}, respectively. Hydrocarbon concentrations inside the chamber, before the injection of the terpene, were below detection limit for all parent terpenes.

2.1. Terpene Compounds and Gas-Phase Measurements

[10] Sixteen different terpenoid compounds were reacted in these experiments: isoprene, eight monoterpenes (α-pinene, β-pinene, 3-carene, terpinolene, α-terpinene, myrcene, limonene, γ-terpinene), four sesquiterpenes (α-humulene, β-caryophyllene, longifolene, and aromadendrene), and three oxygenated terpenes (methyl chavicol, also known as 4-allylanisole, linalool, and verbenone). Table 1 lists the structures and molecular weights of the parent terpenes used and the rate constants for their reactions with OH (k_{OH}). Gas-phase concentrations of the parent terpene were monitored using two instruments: a Hewlett Packard gas chromatograph with a flame ionization detector (GC-FID) using a 60 m × 0.32 μm DB-5 column (J&W Scientific, Davis, CA), and a proton transfer reaction mass spectrometer, or PTR-MS (Ionicon Analytik, Innsbruck, Austria) [*Lindinger et al.*, 1998]. Air from the reaction chamber was sampled using SilcoSteel (Restek Corporation, Bellafonte, PA) tubing, and pulled through a 2 μm pore size PTFE particulate filter (Pall Corportation, East Hills, NY) before analysis by PTR-MS, which measured parent terpenes as well as gas-phase oxidation products. The PTR-MS is a quadrupole mass spectrometer that uses hydronium ions (H_3O^+) to chemically ionize the compound of interest through a proton transfer reaction. Thus, any compound that has a proton affinity higher than that of water can be detected by the PTR-MS, and is identified by its mass to charge ratio (m/z). Because compounds are identified by their molecular weight plus 1 (H^+), the PTR-MS is unable to distinguish between different compounds with the same molecular weight. However, because of the controlled nature of these laboratory chamber experiments, where one terpene at a time is photooxidized, increasing count rates of certain ions are indicative of oxidation products from these reactions. Knowledge of the structures of the parent terpene allows for the deduction of possible identities of the oxidation products from reasonable oxidation mechanisms. However, structurally different oxidation products that have the same mass cannot be distinguished from one another by PTR-MS.

2.2. PTR-MS Calibrations and Concentrations

[11] For calibrations, each pure terpene compound was diluted in cyclohexane and injected into a Teflon bag filled to a final volume of 50 L. Cyclohexane, all parent terpene

Table 2. Molecular Weights Associated With Calibrated Oxidation Products and Sesquiterpenes Detected by PTR-MS

Compound	*m/z* (mass + 1)	Structure	Description
primary signal	21	$H_2{}^{18}OH^+$	isotope of primary ion
	37	$H_2OH_2OH^+$	primary ion water cluster
oxidation	31	CH_2OH^+	formaldehyde
products	45	$C_2H_4OH^+$	acetaldehyde
common to all	47	$CH_2O_2H^+$	formic acid
photooxidation	59	$C_3H_6OH^+$	acetone
experiments	61	$C_2H_4O_2H^+$	acetic acid
β-caryophyllene	*67, 68,* **81**[a]*, 82, 95,* **109**, **121, 137**, **149, 205**, 206	$C_{15}H_{24}H^+$	sesquiterpene, fragments, and isotopes
	85, 113[c]**, 141, 147, 153, 165, 167, 175, 177, 179, 181, 183, 189, 191, 197, 201, 207, 209, 217, 219, 223, 235, 237, 253*[b]		unidentified oxidation products
α-humulene	*67,* **81***, 82, 95, 96, 97, 103,* **109**, *110, 121*, **123,** *135, 137,* **149,** *150,* **205**, 206	$C_{15}H_{24}H^+$	sesquiterpene, fragments, and isotopes
	57, 71, 73, 75, 83, 85, **87***, 89, 99,* **101***, 115, 125, 127, 129, 133, 139, 141, 151*, 153, 155*, 157, 159*, 161, 169*, 175, 179, 183, 191, 193, 209, 219, 223*		unidentified oxidation products
longifolene	*81,* 82, **95**, 96, 103, **109**, 110*, 121, 123, 124, 135, 136,* **149***, 150,* **205***, 206, 207*	$C_{15}H_{24}H^+$	sesquiterpene, fragments, and isotopes
	71, 73, 75, 85, 87, 89, 99, 101, 113, 115, 129, 201,* **203***, 207, 219, 220*[d]*, 221, 223, 235*		unidentified oxidation products
aromadendrene	*95, 96, 103, 109, 110, 121,* **123***, 124,* **135***, 136,* **149***, 150, 163,* **205***, 206, 207*	$C_{15}H_{24}H^+$	sesquiterpene, fragments, and isotopes
	73, 75, 82, 85, 87, 89, 99, 101, 103, 127, 139, 163, 165, **189***, 190*[d]*, 191, 203,* **207***, 209, 219, 221, 222*[d]*, 223*		unidentified oxidation products

[a]Ions associated with parent terpenes listed in bold font represent ions >20% of the unfragmented parent terpene.
[b]Unidentified oxidation products in bold font are ions with >5% yield (on a mole basis) from the parent terpene.
[c]Unidentified oxidation products with asterisks represent ions that were observed at Blodgett Forest using PTR-MS [*Holzinger et al.*, 2005].
[d]Even mass-to-charge ratio oxidation products that are not carbon isotopes of other oxidation products are likely gas-phase nitrogen containing products, e.g., organic nitrates.

compounds, and nopinone were obtained from Fluka Chemicals through Sigma-Aldrich (St. Louis, MO). The monoterpenes were calibrated from the same Teflon bag simultaneously by GC-FID and PTR-MS, and the sesquiterpenes and oxygenated terpenes were only calibrated using PTR-MS. Calibration curves were generated from measurements at three different terpene concentrations. Three different cylinder standards (Scott-Marrin Inc., and Apel-Riemer Environmental Inc.) containing ppm-level concentrations of acetaldehyde, acetone, isoprene, methyl vinyl ketone, methacrolein, and 3-methyl furan were diluted at varying flow rates into the inlet air stream sampling clean compressed air for calibrations of the PTR-MS at three concentration levels ranging from ~50–150 ppb. Three low molecular weight oxidation products: formaldehyde, formic acid, and acetic acid, and nopinone, a higher molecular weight oxidation product from β-pinene oxidation, were calibrated in the PTR-MS using Teflon bags. Nopinone was diluted in cyclohexane before injection into the bag, and the other three oxidation products were diluted in ultrapure water prepared by the Millipore Milli-Q system (Billerica, MA). Two different Teflon bags were used for the calibrations to separate cyclohexane-based and water-based solutions. Cyclohexane and its potential impurities are discussed in more detail by *Lee et al.* [2006]. However, because cyclohexane was only used in the standard calibrations, and not used directly in these photooxidation experiments, no interferences from cyclohexane + OH oxidation products are expected. The standard error of the slope of the calibration curves was <6% for formaldehyde, acetaldehyde, 3-methylfuran, 3-carene, and β-pinene, and <3% for all other terpene compounds and calibrated oxidation products from cylinder standards and Teflon bags. Additional sources of error include the accuracies of the syringe, the volumetric flask used for the terpene dilutions, and the flow controller, together contributing an uncertainty of 3–5%.

[12] The concentrations of compounds for which pure commercial standards were not available were estimated based on the rate constant (k) of the proton transfer reaction, according to the equation [*Lindinger et al.*, 1998]:

$$[R] = \frac{[RH^+]}{[H_3O^+]_0 kt} \quad (1)$$

where $[R]$ is the unknown concentration of the compound of interest, and $[RH^+]$ is the signal of the protonated compound, $[H_3O^+]$ is the primary ion signal, and t is the reaction time in the drift tube. Because the proton transfer reaction rate constants are not known for all compounds, an estimated rate constant (k) of 2×10^{-9} cm^3 molecule^{-1} s^{-1} was used for those compounds without a measured rate constant. The rate constants for the proton transfer reaction of most compounds are generally within ±20% of the estimated k.

[13] Because a pinonaldehyde standard was not available, concentrations were calculated according to Equation (1). Fragments and isotopes associated with pinonaldehyde (Table 2) were determined from correlations with m/z 151 (the dominant pinonaldehyde fragment of the unfragmented m/z 169), and were compared with the fragments reported by *Wisthaler et al.* [2001]. Because our experiments were conducted at a higher drift tube pressure than *Wisthaler et*

Table 3a. Molecular Weights Associated With the Monoterpenes Detected by PTR-MS

Compound	*m/z* (mass + 1)	Structure	Description
limonene	*69,* **81**[a], *82, 95, 96,* **137**, *138*[b]	$C_{10}H_{16}H^+$, $C_6H_9H^+$	monoterpene, fragments and isotopes
	107[c], *108,* **123**[d]*,*124, 133,* **151***, *152, 169*, 170*	$C_{10}H_{16}O_2H^+$	uncalibrated oxidation product: limononaldehyde, fragments, and isotopes
	139, 140	$C_9H_{14}OH^+$	uncalibrated oxidation product: limonaketone and isotope
	57, 69, 70, 71, 73, **75***, 77, 83, 85, 87, 89, 93, 97, 99, 101, 103, 109, 111*, 113*, 115, 121, 125, 127, 129, 131, 135, 141*, 143, 149, 153, 155*, 156, 157, 165, 167, 171, 181, 183, 185, 187, 200*[d]*, 218*[d]		unidentified oxidation products
myrcene	**81**, *82,* **137**, *138*	$C_{10}H_{16}H^+$, $C_6H_9H^+$	monoterpene, fragments and isotopes
	57, 64[e]*, 65,* **71***, 73,* **75***,* **77**, **83**, **85***, 87, 89,* **93***, 97, 99, 101, 103,* **111***, **113***, 115, 125, 127, 129,* **139***, 141, 143, 145, 153, 155*, 159**		unidentified oxidation products
3-carene	**81**, *82,* **137**, *138*	$C_{10}H_{16}H^+$, $C_6H_9H^+$	monoterpene, fragments and isotopes
	107*, 108,* **123***,*124, 133,* **151***, *152, 169*, 170*	$C_{10}H_{16}O_2H^+$	uncalibrated oxidation product: caronaldehyde, fragments, and isotopes
	71, 73, 75, 77, 79, 83, 85, 87, 89, **93***, 94, 97, 99, 101, 103,* **107***, 109, 111*,* 113*, *115, 121,* **123***, *124, 125, 127, 129, 133,* **135**, **139***, **141***, *142,* **151***, **153**, *155*, 157, 167, 169*, 181, 183*		unidentified oxidation products
α-pinene	**81**, *82,* **137**, *138*	$C_{10}H_{16}H^+$, $C_6H_9H^+$	monoterpene, fragments and isotopes
	71*, 72, 99,* **107**, *108,* **109***, 123*, **151**, *152, 169, 170*[f]	$C_{10}H_{16}O_2H^+$	uncalibrated oxidation product: pinonaldehyde, fragments, and isotopes
	69, 73, 75, 83, 85, 87, 89, 94[d]*, 97, 101, 103, 111*, 113*, 115, 121, 125, 127, 129, 131, 139, 141*, 153, 155*, 157, 165, 167, 171, 183, 185, 200*[c]		unidentified oxidation products

[a]Ions associated with parent terpenes listed in bold font represent ions >20% of the unfragmented parent terpene.

[b]All monoterpenes occur predominantly on the parent *m/z* 137 and the fragment *m/z* 81 ions, with a small fraction (<20%) occurring on the ^{13}C isotope with *m/z* (138, 82).

[c]Unidentified oxidation products in bold font are ions with >5% yield (on a mole basis) from the parent terpene.

[d]Unidentified oxidation products with asterisks represent ions that were observed in the canopy air of a coniferous forest in California by PTR-MS [*Holzinger et al.*, 2005].

[e]Even mass-to-charge ratio oxidation products that are not carbon isotopes of other oxidation products are likely gas-phase nitrogen containing products, e.g., organic nitrates.

[f]Fragments were determined from correlations with *m/z* 151 (the dominant pinonaldehyde ion) that also agreed well with fragment ions reported elsewhere for pinonaldehyde [*Wisthaler et al.*, 2001]. Additional fragment ions reported by *Wisthaler et al.* [2001], *m/z* 43 and 81, were excluded from the pinonaldehyde concentration due to interference by other compounds.

al. [2001] (∼2.2 mbar versus ∼2.0 mbar), we expect to observe more fragmentation than reported by *Wisthaler et al.* [2001]. The fragment ions we observed were similar to *Wisthaler et al.* [2001], but *m/z* 151, 152, 169, and 170 represented a smaller proportion of the total pinonaldehyde signal, and *m/z* 43, 72, 99, 108, and 123 represented a larger fraction of the total pinonaldehyde signal. The contribution of the ions *m/z* 71 and 107 were similar to *Wisthaler et al.* [2001]. We did not include the small contribution from *m/z* 81 reported by *Wisthaler et al.* [2001], which was 10% of *m/z* 151, or 3.6% of the total pinonaldehyde signal, because of the interference from α-pinene fragmentation. Additionally, *m/z* 43, 71, and 72 showed time evolutions that deviated from *m/z* 151 towards the end of the experiment, when pinonaldehyde concentrations were decreasing due to further oxidation, suggesting that additional, non-pinonaldehyde compounds were interfering on those mass to charge ratios. Because of the difficulty in determining the pinonaldehyde concentration given the number of fragments and the possibility of interfering compounds, we calculated concentrations in three different ways to estimate a range of likely pinonaldehyde concentrations. The upper limit mixing ratio, which is likely overestimated, is calculated from the sum of concentrations of all pinonaldehyde-associated ions listed in Table 2. The midrange mixing ratio excludes a contribution from *m/z* 43, 71, and 72, which exhibit time evolutions that significantly deviated from *m/z* 151 as pinonaldehyde decreased. The lower-limit mixing ratio, which is probably underestimated, only includes ions (*m/z* 107, 151, 152, 169, 170) that showed the same rate of decrease in signal as *m/z* 151 during the period when pinonaldehyde was undergoing further oxidation. Thus, pinonaldehyde mixing ratios and yields contain a great deal of uncertainty, which is evidenced in the upper and lower-limit range presented in Tables 6 and 9b. Yields of keto-aldehyde compounds from 3-carene, limonene, α-terpinene, and γ-terpinene were determined similarly, from correlations of other product ions with *m/z* 169 and 151. Similar fragment ions were observed (Tables 3a and 3b).

[14] High background counts from the blank chamber air were observed for the low molecular weight oxidation products, resulting in higher detection limits for those

Table 3b. Molecular Weights Associated With the Monoterpenes Detected by PTR-MS

Compound	*m/z* (mass + 1)	Structure	Description
terpinolene	**81**[a], *82,* **137**, *138*	$C_{10}H_{16}H^+$, $C_6H_9H^+$	monoterpene, fragments and isotopes
	65, 71, 73, 75, 77, 83, 85, 86[d], **87**[b], *89,* **93**, *97, 98*[d], **99**, *101, 103, 107, 109,* **111**[c]*, *113*, 115, 123, 125, 126, 127, 129, 135, 141*, 143, 149, 159, 167, 169, 183*		unidentified oxidation products
β-pinene	**81**, *82,* **137**, *138*	$C_{10}H_{16}H^+$, $C_6H_9H^+$	monoterpene, fragments and isotopes
	83, 93, 97, 103, **121**, *122,* **139**, *140, 141**	$C_9H_{14}OH^+$, $C_9H_{12}H^+$	calibrated oxidation product: nopinone, isotopes and fragments
	69, 71, 73, 79, 83, 85, 89, 93, 99, 101, 107, 108[d], *109, 111*, 113*, 115, 123*, 125, 127, 129, 135, 142, 149, 151*, 153, 155*, 157, 165, 167, 169*, 171, 183, 184*[d], *185, 198*[d]		unidentified oxidation products
γ-terpinene	**81**, *82,* **137**, *138*	$C_9H_{14}OH^+$, $C_9H_{12}H^+$	monoterpene, fragments and isotopes
	107, **123***, *124,* **151***, *152,* **169***, *170*	$C_{10}H_{16}O_2H^+$	uncalibrated oxidation product: γ-terpinaldehyde, fragments, and isotopes
	57, 69, 71, 73, 74, 75, 77, 83, 85, **87**, *89,* **93**, *97, 99, 101, 102, 103, 105, 107, 109, 111*, 113*,* **115**, *125, 127, 129, 131, 133,* **135**, *139, 141*, 143, 149, 153, 155*, 157, 159*, 165, 167, 171, 181, 183, 185, 199, 230*[d]		unidentified oxidation products
α-terpinene	*93, 95,* **81**, *82, 135,* **137**, *138*	$C_{10}H_{16}H^+$, $C_6H_9H^+$	monoterpene, fragments and isotopes
	107, **123***, *124,* **151***, *152,* **169***,*170*	$C_{10}H_{16}O_2H^+$	uncalibrated oxidation product: α-terpinaldehyde, fragments, and isotopes
	65, 69, 71, 73, 75, 77, 87, 89, 97, 99, 101, 103, 109, 111, 113*, 115, 125, 127, 129, 131, 135,* **139**, *141*,* **143**, *145, 153, 155*, 157, 158, 159*, 165, 167, 171, 178*[d], *181, 183, 184*[d], *185, 199, 201, 202*[d], *229, 230*[d]		unidentified oxidation products

[a]Ions associated with parent terpenes listed in bold font represent ions >20% of the unfragmented parent terpene.
[b]Unidentified oxidation products in bold font are ions with >5% yield (on a mole basis) from the parent terpene.
[c]Unidentified oxidation products with asterisks represent ions that were observed in the canopy air of a coniferous forest in California by PTR-MS [*Holzinger et al.*, 2005].
[d]Even mass-to-charge ratio oxidation products that are not carbon isotopes of other oxidation products are likely gas-phase nitrogen containing products, e.g., organic nitrates.

compounds. The detection limit ($1\sigma_{\text{background counts}}$/sensitivity) for the monoterpenes was ~70 ppt, for the sesquiterpenes: ~50 ppt, for the oxygenated terpenes: <50 ppt, for nopinone: 20 ppt, for acetaldehyde and acetone: <0.5 ppb, for formic acid: 1.5 ppb, acetic acid: <1 ppb, and for formaldehyde: 6 ppb. Starting concentrations for formaldehyde and formic acid, *m/z* 31 and 47, respectively, were <10 ppb, calculated from count rate divided by the sensitivity of the PTR-MS to those compounds. The background count rate on *m/z* 31 does not result from formaldehyde, but rather from interference from other ions, such as the ^{15}N isotope of NO^+. Additionally, back reactions between protonated formaldehyde (CH_2OH^+) and H_2O make PTR-MS measurements of formaldehyde in ambient air difficult due to low formaldehyde mixing ratios and high water content of ambient air. Formaldehyde was calibrated up to a concentration of ~80 ppb, which was only exceeded in the myrcene (formaldehyde ~110 ppb) and isoprene (formaldehyde >300 ppb) experiments. Thus, our calculated yields of formaldehyde from myrcene and isoprene are subject to significant errors. Mixing ratios of all other oxidation products, from all experiments, were within the calibrated range. Starting concentrations for acetaldehyde, acetone, and acetic acid were <5 ppb. Background counts were subtracted from the signal for ions monitored. Concentrations of the calibrated oxidation products should be considered upper-limit values, as other products with the same molecular weight may occur on the *m/z* of the calibrated products. Thus, the formation of, e.g., glycolaldehyde, is indistinguishable from acetic acid, as they both occur at *m/z* 61.

3. Results and Discussion

[15] Table 1 shows the structures and OH rate constants for the 16 terpenes used. The ions (*m/z*) associated with each parent terpene and their oxidation products are detailed in Tables 2–4. Initial conditions are listed for each experiment in Table 5. The HC:NO_x ratios are reported in Table 5 as ppb C: ppb NO_x, and in Table 6 as ppb HC: ppb NO_x. Hydrocarbon oxidation was initiated primarily by OH, formed from the photodissociation of HONO. Other oxidants, O_3 and NO_3, were also formed, but only later in the experiment, after much of the initial NO is depleted (from reactions with peroxy radicals). This typically occurred after almost all (~80%) of the parent hydrocarbon was depleted, so for most experiments O_3 and NO_3 did not react appreciably with the parent hydrocarbon. Possible exceptions were the sesquiterpenes, β-caryophyllene and α-humulene, which react very rapidly with O_3 [*Shu and Atkinson*, 1994]. Figure 1 shows the time series for O_3, NO, NO_2, and NO_x for a typical experiment (myrcene), where O_3 increases when most of the initial terpene has been depleted, and an

Table 4. Molecular Weights Associated With Other Terpenes Detected by PTR-MS

Compound	*m/z* (mass + 1)	Structure	Description
methyl chavicol	**149**[a], *150*	$C_{10}H_{12}OH^+$	oxygenated terpene and isotope
	65, 71, 73, 75, 85, 89, 97, 99, 101, 103, **109**[b], *113,* **121**, *123*[c]*, 124*[d], *125, 129, 131,* **137**, **151***, *153, 163, 165, 168*[d], *170*[d], *182*[d]		unidentified oxidation products
verbenone	**109**, *110, 123, 133,* **151**, *152*	$C_{10}H_{14}OH^+$	oxygenated terpene, fragments, and isotopes
	69, **71**, *73, 75, 77, 83, 85, 87, 89, 93, 94, 97, 99, 100, 101, 107, 111*, **113***, *115, 123*, 124,* **125**, *127, 129, 130, 141*, 143, 144, 145, 151*, 152, 153, 159*, 167, 169*, 185, 230*[d]		unidentified oxidation products
linalool	**81**, *82,* **137**, *138, 155, 156,*	$C_{10}H_{18}OH^+$, $C_{10}H_{16}H^+$	oxygenated terpene, fragments, and isotopes
	60, **69,** *71, 72, 73, 74,* **75**, *77, 79,* **83**, *85, 87, 89* ,**93**, *97, 99,* **101**, *107,* **111***, *113*, 115, 123*, 124, 125,* **127**, **129**, *141*, 143, 145, 151*, 153, 159*, 167, 169*, 185, 187, 188*[d]		unidentified oxidation products
isoprene	**69**, *70*	$C_5H_8H^+$	isoprene and isotope
	71, *72*	$C_4H_6OH^+$	MVK + MACR
	83, 84	$C_5H_6OH^+$	3-methyl furan
	57, 63, 65, 73, 75, 77, 79, 85, 86, 87, 89, 97, 99, 101, 103, 105, 113, 115, 117, 129, 133*		unidentified oxidation products

[a]Ions associated with parent terpenes listed in bold font represent ions >20% of the unfragmented parent terpene.
[b]Unidentified oxidation products in bold font are ions with >5% yield (on a mole basis) from the parent terpene.
[c]Unidentified oxidation products with asterisks represent ions that were observed in the canopy air of a coniferous forest in California by PTR-MS [*Holzinger et al.*, 2005].
[d]Even mass-to-charge ratio oxidation products that are not carbon isotopes of other oxidation products are likely gas-phase nitrogen containing products, e.g., organic nitrates.

atypical experiment (β-caryophyllene), where O_3 increases after all of the initial terpene has been depleted. The two reactive sesquiterpenes, β-caryophyllene and α-humulene, both show the atypical profile for O_3. This may suggest that the atypical case of delayed O_3 production resulted from titration of O_3 by the parent sesquiterpene and/or first generation oxidation products, which still contain C = C double bonds. For all VOCs, O_3 and NO_3 are expected to react only with unsaturated hydrocarbon oxidation products. Because these products have generally received little study, it is difficult to estimate the relative contributions of OH, O_3, and NO_3 to such chemistry. However, it will be shown for selected terpenes that the formation of most of the major observed oxidation products can be explained using OH chemistry, suggesting that the roles of O_3 and NO_3 reactions are minimal.

[16] Numerous oxidation product ions were produced, many of which have been observed in ambient air within and above Blodgett Forest [*Holzinger et al.*, 2005]. The yields of the oxidation product ions observed in these photooxidation experiments that were also observed by *Holzinger et al.* [2005] are listed in Table 7. In ambient air, *m/z* 113 and 111 were dominant ions, and these ions were observed at low concentrations from all terpenes (*m/z* 113), and from all monoterpenes and a few oxygenated terpenes (*m/z* 111). Yield of *m/z* 113 was highest from myrcene (32%), and yield of *m/z* 111 was highest from terpinolene (29%) and linalool (20%), while aromadendrene did not produce any ions that were observed at Blodgett Forest. The number of oxidation ions observed from these photooxidation experiments is significantly larger than the number of oxidation ions observed from the ozonolysis experiments we conducted previously [*Lee et al.*, 2006]. The mean number of oxidation product ions observed from ozonolysis reactions was 14 ± 5 (mean ± SD) and the mean number of ions observed from photooxidation reactions was 33 ± 6. The PTR-MS was operated under similar conditions for both sets of oxidation experiments, with a drift tube pressure ~2.2 mbar, suggesting that the difference in the number of ions observed is not a result of increased fragmentation of products in the photooxidation experiments. Given the greater versatility of OH attack on the parent terpenes, a greater number of different products formed by photooxidation compared to ozonolysis are expected.

[17] Yields of SOA and gas-phase oxidation products will be discussed according to terpene classification, i.e., sesquiterpenes, monoterpenes, and other terpenes (oxygenated terpenes and isoprene). The gas-phase yields reported in Tables 6–10 were calculated as the slope of the linear least-squares fit of the regression between the product and the parent hydrocarbon. This method was used for both first- and second-generation products. For first-generation products that were further oxidized, only the linear, increasing portion of the regression was considered. Yields of second-generation oxidation products were calculated from a regression line based on an individually-selected time period that most appropriately reflected the production of the individual ion. Although stoichiometric yields of second-generation products are more precisely quantified against their parent compound (the first-generation product oxidized to produce the second-generation product), because first-generation products are generally unidentified, and because the parent terpenes are more commonly and easily measured than first-generation products in the real atmosphere, we report yields of second-generation products as a function of the parent terpenes, rather than their first-generation precursors. The carbon balance was calculated for each experiment as a function of time, and is represented in Figure 2 as an average for a 30–60 minute snapshot at the middle or end of each experiment for the purpose of carbon counting, and does not represent overall the stoi-

Table 5. Comparison of SOA Yields Obtained From This Study With Results From Other Photooxidation Experiments

Terpene	Temp, K	RH, %	ΔHC, ppb	ΔM_o, μg m^{-3}	HC:NO_x, ppbC/ppb	SOA Mass Yield,[g] %	Reference
β-caryophyllene	**295**	**56**	**37 ± 3**	**212 ± 2**	**19**	**68 ± 7**	**This work**
	319[d]			845, 998	9	103, 125	[*Hoffmann et al.*, 1997]
	308, 309			17–82	3, 8	37–79[b]	[*Griffin et al.*, 1999]
α-humulene	**294**	**53**	**46 ± 1**	**254 ± 2**	**20**	**65 ± 1**	**This Work**
	308, 307			13–59	3	32–85[b]	[*Griffin et al.*, 1999]
longifolene	**293**	**49**	**34 ± 2**	**186 ± 2**	**9**	**65 ± 1**	**This work**
limonene	**294**	**45**	**120 ± 2**	**394 ± 4**	**11**	**58 ± 1**	**This Work**
	313, 309			10–120	2, 5	8.7–34	[*Griffin et al.*, 1999]
						4.3[f]	[*Larsen et al.*, 2001]
Myrcene	**294**	**53**	**112 ± 2**	**272 ± 3**	**9**	**43 ± 1**	**This Work**
	311, 312			3.5, 57.5	2, 4	5.6–6.8	[*Griffin et al.*, 1999]
methyl chavicol	**294**	**49**	**79 ± 2**	194 ± 2	**8**	**40 ± 1**	**This work**
3-carene	**294**	**52**	**109 ± 2**	**236 ± 3**	**8**	**38 ± 1**	**This work**
	319, 312[d]			143, 161	10	23, 27	[*Hoffmann et al.*, 1997]
	310, 312			2.5–99.7	3, 7	2–18[b] 0.5[f]	[*Griffin et al.*, 1999]
						0.5[f]	[*Larsen et al.*, 2001]
aromadendrene	**294**	**47**	**34 ± 1**	**107 ± 2**	**21**	**37 ± 2**	**This work**
α-pinene	**293**	**43**	**109 ± 1**	**199 ± 3**	**12**	**32 ± 0.1**	**This work**
	298			not given		4–40[c]	[*Noziere et al.*, 1999]
	?			?		43	[*Hatakeyama et al.*, 1991]
	309–324			1–96	7–15[a]	43 1–12[d]	[*Hoffmann et al.*, 1997]
						~32–45[e]	[*Jaoui and Kamens*, 2001]
						1.8[f]	[*Larsen et al.*, 2001]
terpinolene	**294**	**50**	**110 ± 5**	**190 ± 4**	**11**	**31 ± 2**	**This Work**
	313, 316			25–133	3, 4	1.5–4.1	[*Griffin et al.*, 1999]
β-pinene	**293**	**50**	**170 ± 5**	**293 ± 4**	**21**	**31 ± 1**	**This work**
	307–317			153	9[a]	30	[*Hoffmann et al.*, 1997]
	297–304				21.1	20.9	[*Jaoui and Kamens*, 2003b]
	316, 313			7–141	7, 6	3–27[b]	[*Griffin et al.*, 1999]
						1.8[f]	[*Larsen et al.*, 2001]
γ-caryophyllene	**294**	**48**	**118 ± 6**	**193 ± 3**	**11**	**29 ± 2**	**This Work**
	312, 311			21, 66	5, 4	9.8–16	[*Griffin et al.*, 1999]
α-terpinene	**293**	**47**	**103 ± 1**	**145 ± 1**	**9**	**25 ± 0.4**	**This Work**
	316, 313			20, 74	3, 5	8.2–17.5	[*Griffin et al.*, 1999]
Verbenone	**294**	**46**	**105 ± 2**	**127 ± 2**	**11**	**19 ± 0.4**	**This work**
linalool	**295**	**40**	**124 ± 2**	**104 ± 4**	**10**	**13 ± 0.3**	**This work**
	320, 318[d]			19, 137	11, 9	4.2, 9.8	[*Hoffmann et al.*, 1997]
	312			26.7	2	5.6	[*Griffin et al.*, 1999]
isoprene	**294**	**54**	**506 ± 33**	**26 ± 1**	**9**	**2 ± 0.1**	**This work**
	~293	~50	25–500	0.5–30	0.1–1.8	1–3	[*Kroll et al.*, 2005]

[a]The reported hydrocarbon to NO_x ratio includes propene, used as the photochemical initiator.

[b]The range reported here represent the lowest and highest yields from a series of experiments, with the corresponding temperatures, ΔM_o, and hydrocarbon to NO_x ratios.

[c]Assumed aerosol density of 1 g cm^{-3}. The range of aerosol yield results from several different experiments with higher yields observed from higher initial α-pinene concentrations.

[d]From nine different experiments. Average of reported range of temperatures.

[e]Aerosol yields are reported as the maximum carbon yield (19–27%). To convert to total SOA mass yield for comparison with other experiments, we assumed the aerosol was 60% carbon.

[f]Percent molar yield of identified carboxylic acids and carbonyls in the aerosol phase.

[g]SOA yields are expressed on a percent mass basis, using the ratio of μg organic aerosol m^{-3} to μg parent terpene m^{-3}, assuming an aerosol density of 1.25 g cm^{-3}.

chiometric yields (Tables 6–10). The estimated carbon balance from all experiments ranged from 52 ± 5% to 138 ± 55%, with considerable uncertainties associated with the assignment of carbon number for each unidentified ion, as well as uncertainty from the calibration of parent terpenes and oxidation products, and the collisional rate constant. Although we assumed SOA was 60% carbon (based on the %C of pinic acid), this number is uncertain and may vary for each experiment, and likely affected the total carbon balance by elevating it, resulting in carbon balances for some experiments >100%. The carbon balances for each experiment are shown in Figure 2, and because of the large uncertainty associated with the mass balance, reflect a qualitative assessment of the ability of the PTR-MS to detect the unidentified compounds according to their *m*/*z*. Clearly, the products formed from sesquiterpene photooxidation are not as readily detected by PTR-MS as the products from the photooxidation of other terpenes.

[18] Product yields from other studies are also compared with the results obtained from these experiments (Tables 8 and 9a–9c), however, other experiments often use different radical precursors, such as CH_3ONO, NO_2, or H_2O_2, which may impact gas-phase and SOA yields. Thus, these comparisons are included to simply present the range of yields observed elsewhere under different experimental conditions. In addition to carbonyls and acids, these photooxidation experiments in the presence of NO_x should be expected to produce organic nitrates. Theoretical calculations have sug-

Table 6. Gas-Phase Yields From Terpene Photooxidation Experiments

Terpene	$\frac{HC}{NO_x}$[a]	CH_2O[b] % Yield	C_2H_4O % Yield	CH_2O_2 % Yield	C_3H_6O % Yield	$C_2H_4O_2$ % Yield	UnID[c] % Yield	Total C Balance,[d] %
β-caryophyllene	1.3	**42 ± 10**	0.6 ± 0.2	6.2 ± 2	1.5 ± 0.4	8.7 ± 2	22 ± 1	62 ± 5
α-humulene	1.4	—	0.2 ± 0.1	6.1 ± 0.8	2.4 ± 0.3	7.5 ± 0.7	54 ± 3	77 ± 9
longifolene	0.8	**25 ± 3**	3.7 ± 0.4	**31 ± 3**	3.8 ± 0.3	15 ± 1	30 ± 2	62 ± 7
limonene	1.1	**43 ± 5**	0.7 ± 0.1	5.0 ± 0.6	0.4 ± 0.1	3.2 ± 0.4	61 ± 3[e]	113 ± 17
myrcene	0.9	**74 ± 8**[f]	0.7 ± 0.1	4.5 ± 0.5	**22 ± 2**	3.9 ± 0.4	134 ± 10	100 ± 17
methyl chavicol	0.8	**52 ± 6**	0.7 ± 0.1	7.9 ± 1	0.7 ± 0.1	**25 ± 2**[g]	121 ± 11	101 ± 20
3-carene	0.8	**35 ± 4**	1.6 ± 0.2	5.4 ± 0.6	9.3 ± 0.9	5.1 ± 0.6	95 ± 5[h]	138 ± 55
aromadendrene	1.4	**65 ± 8**	2.9 ± 0.3	12 ± 2	4.8 ± 0.5	4.1 ± 0.4	69 ± 7	74 ± 14
α-pinene	1.1	16 ± 2	1.4 ± 0.2	4.5 ± 0.5	6.3 ± 0.6	3.4 ± 0.4	91 ± 14[i]	100 ± 7
terpinolene	1.1	**23 ± 3**	0.7 ± 0.1	3.5 ± 0.7	**20 ± 2**	1 ± 0.2	109 ± 8	87 ± 18
β-pinene[j]	2.1	**49 ± 6**	0.6 ± 0.1	8.2 ± 0.7	7.9 ± 0.7	1.4 ± 0.1	26 ± 1	52 ± 5
γ-terpinene	1.1	17 ± 2	1.2 ± 0.2	8.3 ± 0.8	5.3 ± 0.5	4.5 ± 0.5	130 ± 10[k]	112 ± 28
α-terpinene	1.0	7.8 ± 2	0.7 ± 0.1	6.1 ± 1	3.1 ± 0.4	2 ± 0.3	61 ± 4[l]	123 ± 40
verbenone	1.1	**32 ± 2**	2.1 ± 0.3	8 ± 0.8	13 ± 1	6.9 ± 0.6	92 ± 4	79 ± 17
linalool	1.0	**43 ± 5**	1.1 ± 0.1	3.2 ± 0.4	**25 ± 2**	17 ± 2[g]	144 ± 11	104 ± 25
isoprene[m]	1.8	**160 ± 19**[f]	1.9 ± 0.3	4.6 ± 0.6	0.4 ± 0.1	5.7 ± 0.7[g]	15 ± 1	101–114 ± 22

[a]Initial hydrocarbon (ppb parent terpene) to NO_x (ppb NO + NO_2) ratio of the experiment.
[b]Gas-phase yields of CH_2O (formaldehyde), C_2H_4O (acetaldehyde), CH_2O_2 (formic acid), C_3H_6O (acetone), and $C_2H_4O_2$ (acetic acid), are expressed on a percent mole basis. Product yields >20% are listed in bold.
[c]Unidentified molar yields does not include the identified but uncalibrated ions associated with the dominant aldehydes formed from limonene, 3-carene, α-pinene, α-terpinene, and γ-terpinene (Table 2).
[d]Total carbon balance calculated from the sum of the gas-phase products and SOA, assuming aerosol is 60% carbon. See text for explanation of uncertainty estimates.
[e]Yield of limononaldehyde was 68 ± 7%.
[f]Subject to significant error due to concentrations beyond range of calibrations.
[g]Likely includes a contribution from glycolaldehyde ($C_2H_4O_2$, MW = 60).
[h]Molar yield of caronaldehyde was 77 ± 8%.
[i]The midrange pinonaldehyde yield was used in the calculation.
[j]The nopinone yield from β-pinene photooxidation was 17 ± 2%.
[k]Yield of γ-terpinaldehyde was 57 ± 6%.
[l]Yield of α-terpinaldehyde was 19 ± 2%.
[m]MVK + MACR yield was 60–87 ± 11% and 3-methylfuran yield was 3.6 ± 0.4%.

gested that OH oxidation of α-pinene produces a 19% yield of organic nitrates in chamber experiments, and a 13% yield in the real atmosphere [*Peeters et al.*, 2001]. Laboratory experiments have suggested that abstraction from aldehydic H on pinonaldehyde produces high yields (81%) of a PAN analogue under high NO_x conditions [*Noziere and Barnes*, 1998]. Table 10 lists the molar yields of the even *m*/*z* product ions (characteristic of a N-containing compound), which were produced from ten of the terpene compounds at extremely low yields. The PTR-MS observed a 1% yield of organic nitrates from α-pinene, suggesting that perhaps these organic nitrates were thermally unstable in the PTR-MS, fragmented in the PTR-MS on odd *m*/*z*, which are not typically associated with N-containing compounds, were lost to tubing walls, or were not formed at high yields in these experiments. If these organic nitrates are high carbon number compounds, such as the PAN analogue from pinonaldehyde oxidation, then the poor detection of these compounds by PTR-MS should affect the carbon mass balance of the experiments. Poor carbon balances were obtained for β-pinene and the sesquiterpenes, and undetected organic nitrates may be responsible. However, due to the high degree of uncertainty in the carbon mass balance, a 20% yield of undetected organic nitrates are within the uncertainty estimates of many of the experiments, and may not represent a significant and detectable carbon loss.

[19] Time series graphs and production mechanisms for selected ions from selected terpenes will be presented, and will focus primarily on *m*/*z* 113 and 111. The production mechanisms for many of the product ions are very straightforward, however, in order to generate compounds that correspond with the observed product ions and time series, many of the production mechanisms represent pathways that seem less likely or straight-forward. In the following sections, we suggest possible mechanisms and products for a limited number of terpenes and their observed ions that correspond best to the observed data, focusing primarily on the ions observed in a ponderosa pine forest canopy [*Holzinger et al.*, 2005], while also addressing the inconsistencies between expected and observed ions. Aerosol yields and comparisons with other studies are presented in Table 5, but a more detailed analysis of the contribution of first- and second-generation oxidation products to SOA production from these photooxidation experiments, and ozonolysis experiments performed in 2003 [*Lee et al.*, 2006], is presented elsewhere [*Ng et al.*, 2006].

3.1. Sesquiterpenes

[20] SOA yields were highest from β-caryophyllene (68%), α-humulene (65%), and longifolene (65%), with an intermediate SOA yield of 37% from aromadendrene (Table 5). The relatively few experiments conducted on sesquiterpene oxidation have focused primarily on β-caryophyllene and α-humulene, thus no data was found in the existing literature on longifolene and aromadendrene photooxidation. High SOA yields for β-caryophyllene and α-humulene have been observed by other studies [e.g.,

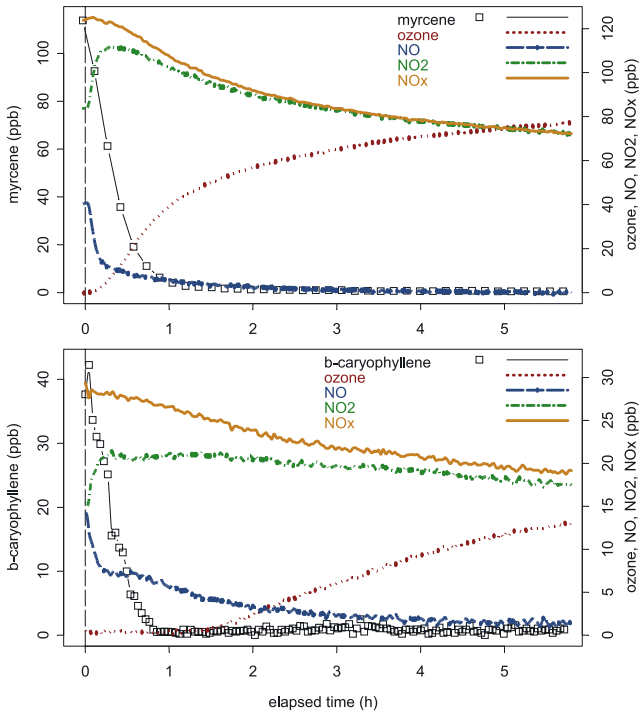

Figure 1. Time series plots of O_3, NO, NO_2, and NO_x for myrcene, which was fairly representative of all experiments, and β-caryophyllene, which was similar to α-humulene, but atypical compared to all other experiments. Red dotted lines represent O_3. Blue dashed lines represent NO. Green dotted and dashed lines represent NO_2. Orange solid lines represent NO_x.

Hoffmann et al., 1997; *Griffin et al.*, 1999]. Gas-phase yields of low molecular weight oxidation products (Table 6) varied for the sesquiterpenes, with high formaldehyde yields from aromadendrene, β-caryophyllene, and longifolene, all with an external double bond, and relatively low yields of acetaldehyde, acetone, and acetic acid. High formic acid yields were observed from longifolene, but not from β-caryophyllene or aromadendrene, all with external double bonds. The carbon mass balances for all four sesquiterpenes are relatively low compared to most other monoterpenes, ranging from 62–77%. The poor mass balances for the sesquiterpenes suggests that the observed unidentified products are underestimated or that additional gas-phase products were formed that were not measured by PTR-MS.

3.1.1. Aromadendrene and Longifolene

[21] The photooxidation of aromadendrene produced high yields of *m/z* 207 and 189 (47 ± 7%), which are likely the dominant product ions of the ketone formed from OH addition at the terminal carbon of the external double bond. The formation of this product would also produce formaldehyde, which also accounts for the high formaldehyde yield observed (65 ± 8%). In contrast, the photooxidation of longifolene, which is similar in structure to aromadendrene, produced low yields of *m/z* 207 (2 ± 0.4%), and *m/z* 189 was not observed. Yields of formic acid were greater than formaldehyde, and the dominant unidentified ion produced was *m/z* 203, at a yield of only 5 ± 1%, suggesting that the photooxidation of longifolene is more complex than that of aromadendrene, with several different pathways that produce lower gas-phase yields of many different products and higher yields of SOA, which is surprising given that the similar, and comparatively simple structures of these two sesquiterpenes would suggest similar oxidation pathways and yields.

3.1.2. α-Humulene

[22] The photooxidation of α-humulene, with no external double bonds, did not produce formaldehyde, and produced low yields of the other calibrated oxidation products. Initial oxidation of any one of the three internal double bonds would produce a high molecular weight C_{15} multifunctional species (e.g., a $C_{15}H_{24}O_2$ keto-aldehyde occurring at *m/z*

Table 7. Percent Yield (Slope of Regression ± Standard Error of Slope) on a Mole Basis, of Product Ions From Terpene Photooxidation That Were Also Observed in the Ambient Air Within a Ponderosa Pine Canopy in California

Terpene	*m/z* 111	*m/z* 113	*m/z* 123	*m/z* 141	*m/z* 151	*m/z* 155	*m/z* 159	*m/z* 169
β-caryophyllene[a]		*0.4 ± 0.1*		*0.4 ± 0.1*				
α-humulene[a]		*1.1 ± 0.3*		*1.1 ± 0.2*	*1.5 ± 0.3*		*0.3 ± 0.1*	*0.5 ± 0.2*
longifolene		*0.7 ± 0.1*						
limonene	1 ± 0.2	1 ± 0.2	**21 ± 4**[b]	1.3 ± 0.3	**13 ± 3**	0.7 ± 0.2	0.1 ± 0.02	4.6 ± 1
myrcene	**9.3 ± 2**[c]	**32 ± 7**	5.5 ± 1	0.6 ± 0.2		1.1 ± 0.3	0.1 ± 0.02	
3-carene	1.7 ± 0.4	2 ± 0.4	**26 ± 6**	4.5 ± 1	**19 ± 4**	0.8 ± 0.2		6.9 ± 2
methyl chavicol		0.9 ± 0.1	0.5 ± 0.04		**23 ± 0.4**			
α-pinene	1 ± 0.2	0.9 ± 0.2	3.6 ± 0.7	1 ± 0.2	**24 ± 5**	0.8 ± 0.2		2.4 ± 0.5
terpinolene	**29 ± 6**[d]	2.8 ± 0.6	1.7 ± 0.4	1.7 ± 0.4				
β-pinene	0.7 ± 0.2	0.4 ± 0.1	1.1 ± 0.2		1.4 ± 0.3	0.8 ± 0.2		
γ-terpinene	0.4 ± 0.1	1 ± 0.2	**17 ± 4**	2.2 ± 0.5	**14 ± 3**	0.7 ± 0.1	0.1 ± 0.02	**14 ± 3**
α-terpinene	0.6 ± 0.1	0.6 ± 0.2	7.2 ± 2	0.9 ± 0.4	4.6 ± 1	3.4 ± 1	0.1 ± 0.03	2.7 ± 1
verbenone[a]	*3.2 ± 0.7*	*6.5 ± 1*		*1.8 ± 0.4*		*1.5 ± 0.3*	*0.2 ± 0.04*	*0.4 ± 0.1*
linalool[a]	***20 ± 4***[e]	*2.5 ± 0.5*	*0.7 ± 0.1*	*0.5 ± 0.1*	*0.4 ± 0.1*		*0.04 ± 0.02*	*0.3 ± 0.1*
isoprene		*0.6 ± 0.1*						

[a]The terpenes listed in italic font have not been measured in the air above the Blodgett Forest canopy. The short lifetime of the two sesquiterpenes, β-caryophyllene and α-humulene likely affect their detection in ambient air above the canopy, and linalool, typically associated with flowering citrus plants, may not be emitted at all from Blodgett Forest. Verbenone, an oxygenated terpene associated with plant-insect interactions, has not been specifically targeted for measurements at Blodgett Forest.

[b]Yields listed in bold are yields greater than 10%, and all yields of unidentified product ions represent a lower limit due to lack of knowledge about fragmentation.

[c]Yield of *m/z* 111. The sum of yields of *m/z* 111 and 93 is 41 ± 7% (see text).

[d]Yield of *m/z* 111. Sum of yields of *m/z* 111 and 93, the dehydrated fragment of *m/z* 111, was 43 ± 7%.

[e]Yield of *m/z* 111. The sum of yields of *m/z* 129, 111 and 93 is 75 ± 10%.

Table 8. Comparison of Gas-Phase Oxidation Product Yields From Sesquiterpenes, Isoprene, and Oxygenated Terpenes, on a Percent Mole (ppb/ppb) Basis, Observed in This Study With Results From Other Terpene Photooxidation Experiments

Terpene	Product	Product Yield, % This Work	Product Yield, % Other Studies	Reference
α-humulene	*m/z* 219	3 ± 0.5	9.5[a]	[*Jaoui and Kamens*, 2003a]
linalool	acetone	25	51	[*Shu et al.*, 1997]
	m/z 127	8.1 ± 2	6.8[b]	[*Shu et al.*, 1997]
	m/z 129, 111, 93	75 ± 10	46[c]	[*Shu et al.*, 1997]
isoprene	formaldehyde	160[d]	63 ± 10	[*Tuazon and Atkinson*, 1990]
			57 ± 6	[*Miyoshi et al.*, 1994]
	MVK + MACR	60–87 ± 11	61	[*Paulson et al.*, 1992]
			55 ± 6	[*Zhao et al.*, 2004]
			54	[*Tuazon and Atkinson*, 1990]
			54	[*Miyoshi et al.*, 1994]
	3-methylfuran	3.6 ± 0.4	4.4 ± 0.6	[*Atkinson et al.*, 1989]
			4 ± 2	[*Paulson et al.*, 1992]
			<2	[*Sprengnether et al.*, 2002]
	m/z 85	1.5 ± 0.3	8.4 ± 2.4[e]	[*Zhao et al.*, 2004]
	m/z 87	1.3 ± 0.3	3.3 ± 1.6[f]	[*Zhao et al.*, 2004]
	m/z 101	0.5 ± 0.1	∼15%[g]	[*Baker et al.*, 2005]
			19.3 ± 6.1[h]	[*Zhao et al.*, 2004]

[a]Sum of yields of 3-seco-α-humulone aldehyde and 7-seco-α-humulone aldehyde, and α-humulal aldehyde, all with MW = 236. We did not observe *m/z* 237, but did observe *m/z* 219, its dehydrated fragment.
[b]Yield of 6-methyl-5-hepten-2-one ($C_8H_{14}O$ = 126 amu).
[c]Yield of 4-hydroxy-2-methyl-5-hexen-1-al and its cyclized isomer ($C_7H_{12}O_2$ = 128 amu).
[d]Likely overestimated due to calibration issue.
[e]Yield of *m/z* 85 measured by PTR-MS and attributed to a C_5 carbonyl (C_5H_8O = 84 amu).
[f]Yield of *m/z* 87 measured by PTR-MS and attributed to a C_4 hydroxycarbonyl ($C_4H_6O_2$ = 86 amu).
[g]Estimated yield of two C_5 hydroxycarbonyls.
[h]Yield of *m/z* 101 measured by PTR-MS and attributed to a C_5 hydroxycarbonyl ($C_5H_8O_2$ = 100 amu).

237), however, this ion was not observed from α-humulene photooxidation, suggesting that this species was not detected because it was rapidly oxidized, partitioned directly into the particle phase, or fragmented completely in the PTR-MS. Additionally, higher yields of lower molecular weight unidentified ions, e.g., *m/z* 87, 99, 101, and 125 were observed, indicating ring-opening did occur with cleavage at multiple internal double bonds. Despite the higher yields of comparatively low molecular weight ions, SOA yield from α-humulene was still high. The gas- and particle-phase products from the photooxidation of α-humulene was studied elsewhere [*Jaoui and Kamens*, 2003a] using denuder and filter sampling with sample derivatization and analysis by GC-MS and HPLC. By accounting for nine different oxidation products in the gas and particle phases, *Jaoui and Kamens* [2003a] obtained a carbon balance of ∼44%, suggesting that the use of surrogate standards underestimated yields, or that additional products may be produced. In the gas-phase, carbon yields of 3-seco-α-humulone aldehyde, 7-seco-α-humulone aldehyde, and α-humulal aldehyde (all MW = 236) dominated, and summed to 9.5% [*Jaoui and Kamens*, 2003a]. Although we did not observe a product ion at *m/z* 237, we did observe *m/z* 219, which is expected to be the dehydrated fragment of *m/z* 237. Our observed yield of *m/z* 219 (3 ± 0.5%) was lower than the sum of the three C_{15} products observed by *Jaoui and Kamens* [2003a], which is expected as these compounds likely produce additional fragments or are otherwise lost to tubing walls. Our carbon mass balance for α-humulene was 77 ± 9%, suggesting that the gas-phase compounds observed by PTR-MS as 32 product ions, though underestimated, likely include additional products besides the nine identified by *Jaoui and Kamens* [2003a].

3.1.3. β-Caryophyllene

[23] Figure 3 shows the time series of β-caryophyllene photooxidation, indicating that the production of *m/z* 207 occurs quickly, corresponding to OH addition to the terminal C of the external double bond (Figure 4). Oxidation products with MW = 236 and 252 have been proposed for β-caryophyllene ozonolysis [*Calogirou et al.*, 1997], and represent first-generation oxidation products from O_3 attack at the internal double bond. Although OH attack at the internal double bond would also likely result in first-generation products occurring at *m/z* 237 and 253 (Figure 4), the observed time evolution and mixing ratio of *m/z* 237 suggest that this ion corresponds to a non-dominant, late-forming (perhaps third-generation) product. It is possible that the first-generation keto-aldehyde product corresponding to *m/z* 237 was formed but not observed in the gas-phase because it partitioned directly into the particle phase. The formation of oxidation products at *m/z* 253 and 235 is observed but delayed compared to *m/z* 207 and 189 (Figure 3). While *m/z* 189 may be the dehydrated fragment of *m/z* 207, the time series of the two ions are not identical (Figure 2) and the correlation coefficient is low (R^2 = 0.3), suggesting that *m/z* 189 is a different product, or that the very low mixing ratios observed for *m/z* 189 and 207 makes a correlation difficult to detect. Figure 4 shows partial mechanisms for the initial production and further oxidation of *m/z* 207. For comparison, the first-generation products corresponding to MW = 236 and 252, proposed by *Calogirou et al.* [1997], that are not likely the products observed in these photooxidation experiments, are illustrated in grey. The further oxidation of *m/z* 207 may produce the observed oxidation ions *m/z* 219, 237, the dehydrated fragments of *m/z* 255 (Figure 4). Although the

Table 9a. Comparison of Gas-Phase Oxidation Product Yields From Monoterpenes, on a Percent Mole (ppb/ppb) Basis, Observed in This Study With Results From Other Terpene Photooxidation Experiments

Terpene	Product	Product Yield, % This Work	Product Yield, % Other Studies	Reference
limonene	Formaldehyde	43	92[a]	[*Librando and Tringali*, 2005]
			36 ± 5[a]	[*Larsen et al.*, 2001]
	formic acid	7	54 ± 10[a]	[*Larsen et al.*, 2001]
			54[a]	[*Librando and Tringali*, 2005]
	Acetone	0.4	<0.03	[*Reissell et al.*, 1999]
			not detected	[*Larsen et al.*, 2001]
	m/z 139[b]	4.9 ± 1	39 ± 15[c]	[*Larsen et al.*, 2001]
			20 ± 3	[*Hakola et al.*, 1994]
			17 ± 3	[*Arey et al.*, 1990]
	m/z 169[d]	68 ± 7	29 ± 6[e]	[*Hakola et al.*, 1994]
			28	[*Arey et al.*, 1990]
			not detected	[*Larsen et al.*, 2001]
myrcene	Formaldehyde	74[f]	30 ± 6	[*Orlando et al.*, 2000]
	formic acid	5	5 ± 2	[*Orlando et al.*, 2000]
	Acetone	22	36 ± 5	[*Orlando et al.*, 2000]
			41	[*Reissell et al.*, 1999]
	m/z 111	9.3 ± 2	19 ± 4[g]	[*Reissell et al.*, 2002]
3-carene	Formaldehyde	35	21 ± 4	[*Orlando et al.*, 2000]
			12 ± 3	[*Larsen et al.*, 2001]
			20[a]	[*Librando and Tringali*, 2005]
	formic acid	5	30 ± 3 11[a]	[*Larsen et al.*, 2001]
			11[a]	[*Librando and Tringali*, 2005]
			8 ± 2	[*Orlando et al.*, 2000]
	Acetone	9	15 ± 3	[*Orlando et al.*, 2000]
			15 ± 3	[*Reissell et al.*, 1999]
	Acetone		15 ± 5	[*Larsen et al.*, 2001]
	m/z 169	77 ± 8[h]	34 ± 8[i]	[*Hakola et al.*, 1994]
			31[i]	[*Arey et al.*, 1990]
			14 ± 5[i]	[*Larsen et al.*, 2001]

[a]From experiments where the photolysis of H_2O_2 was used as the OH source.
[b]Sum of *m/z* 139 and 121.
[c]Yield of limona ketone.
[d]Sum of yields of *m/z* 169, 170, 151 (the dehydrated fragment of *m/z* 169), 152, 133, 123, 124, 107, and 108.
[e]Yield of endolim, also called limononaldehyde.
[f]Subject to significant error due to concentrations beyond range of calibrations.
[g]Yield of 4-vinyl-4-pentenal.
[h]Sum of *m/z* 169, 170, 151 (the dehydrated fragment of *m/z* 169), 152, 133, 123, 124, 107, and 108.
[i]Yield of caronaldehyde.

production of a keto-keto-aldehyde from further oxidation of *m/z* 207 at the remaining internal double bond, with a molecular weight of 238 (*m/z* 239) seems likely, the ions *m/z* 239 and 221, which are shown for reference in Figure 4, were not observed from these experiments. It should also be noted that many products, particularly the acids, may also be produced from ozonolysis reactions.

[24] We conducted dark ozonolysis experiments of β-caryophyllene and α-humulene in 2003 [*Lee et al.*, 2006], and in comparison, the photooxidation of these two sesquiterpenes produced higher SOA yields than ozonolysis. Because the lifetime of these two sesquiterpenes from O_3 reaction is considerably shorter compared to OH oxidation, the lower SOA yields of ~45% from ozonolysis may be atmospherically relevant.

3.2. Monoterpenes

[25] SOA yields from monoterpenes ranged from 25% to 58% (Table 5). Yields are generally expected to be higher from terpenes with internal double bonds, because oxidation does not necessarily result in carbon loss. This trend is generally observed, with several terpenes with internal double bonds, such as limonene, 3-carene, α-pinene, and terpinolene, producing higher SOA yields than β-pinene, the only single external double bond monoterpene tested. However, high SOA yields were observed from myrcene, which is acyclic, and low SOA yields were observed from α- and γ-terpinene, both with two internal double bonds.

3.2.1. Limonene

[26] The 58% SOA yield from limonene was highest of all monoterpenes (Table 5). High yields of formaldehyde were also observed from limonene, whereas yields of acetaldehyde, formic acid, acetone, and acetic acid were low. Limononaldehyde ($C_{10}H_{16}O_2$) has been reported as a limonene oxidation product [*Hakola et al.*, 1994], and the PTR-MS observed high yields of the ions we determined to be associated with limononaldehyde (Table 3a), with a total yield of 68 ± 7%. In comparison to other studies (Table 9a), we observed a very high yield of limononaldehyde and low yields of limonaketone, formaldehyde, and formic acid. The time series of limonene photooxidation is shown in Figure 5. Limononaldehyde and limonaketone were observed simultaneously, but higher yields of limononaldehyde suggest OH preferentially attacks limonene at the internal double bond. Other ions are subsequently produced, and are likely oxidation products of limononaldehyde, such

Table 9b. Comparison of Gas-Phase Oxidation Product Yields From Monoterpenes, on a Percent Mole (ppb/ppb) Basis, Observed in This Study With Results From Other Terpene Photooxidation Experiments

Terpene	Product	Product Yield, % This Work	Product Yield, % Other Studies	Reference
α-pinene	formaldehyde	16	23 ± 9	[*Noziere et al.*, 1999]
			19 ± 5	[*Orlando et al.*, 2000]
			16[a]	[*Librando and Tringali*, 2005]
			8 ± 1[b]	[*Noziere et al.*, 1999]
			8 ± 1[a]	[*Larsen et al.*, 2001]
	formic acid	5	28 ± 3	[*Larsen et al.*, 2001]
			13[a]	[*Librando and Tringali*, 2005]
			7 ± 2	[*Orlando et al.*, 2000]
	acetone	6	15 ± 2	[*Wisthaler et al.*, 2001]
			11 ± 3	[*Reissell et al.*, 1999]
			11 ± 3[a]	[*Larsen et al.*, 2001]
			11 ± 3	[*Aschmann et al.*, 1998]
			9 ± 6	[*Noziere et al.*, 1999]
			7 ± 2[b]	[*Noziere et al.*, 1999]
			5 ± 2	[*Orlando et al.*, 2000]
	pinonaldehyde	63 (range 47–83)[c]	87 ± 20	[*Noziere et al.*, 1999]
		30 ± 0.3[d]	56 ± 4	[*Hatakeyama et al.*, 1991]
			37 ± 7[b]	[*Noziere et al.*, 1999]
			34 ± 9	[*Wisthaler et al.*, 2001]
			31 ± 15	[*Vinckier et al.*, 1998]
			31–34[e]	[*Jaoui and Kamens*, 2001]
			29	[*Arey et al.*, 1990]
			28	[*Hakola et al.*, 1994]
			28 ± 5	[*Aschmann et al.*, 2002]
			6 ± 2[a]	[*Larsen et al.*, 2001]
	m/z 153	2.9 ± 0.6	1.4–1.8[f, g]	[*Jaoui and Kamens*, 2001]
	m/z 155	0.8 ± 0.2	4–6.4[f, h]	[*Jaoui and Kamens*, 2001]
	m/z 171	0.2 ± 0.05	3.9–4.2[f, i]	[*Jaoui and Kamens*, 2001]
	m/z 185	0.3 ± 0.1	6.1–16.9[f, j]	[*Jaoui and Kamens*, 2001]
			19[w]	[*Aschmann et al.*, 2002]
terpinolene	formaldehyde	23	29 ± 6	[*Orlando et al.*, 2000]
	formic acid	4	8 ± 2	[*Orlando et al.*, 2000]
	acetone	20	39 ± 5	[*Orlando et al.*, 2000]
			36–45	[*Reissell et al.*, 1999]
	m/z 111 and 93	43 ± 7	26 ± 6[k]	[*Hakola et al.*, 1994]
			26 ± 5	[*Reissell et al.*, 1999]
			24	[*Arey et al.*, 1990]
			19 ± 4[l]	[*Reissell et al.*, 2002]
	m/z 169	—	10	[*Arey et al.*, 1990]

[a]From experiments where the photolysis of H_2O_2 was used as the OH source.
[b]Conducted in the absence of NO_x.
[c]See Experiment section for description of the pinonaldehyde yield calculation.
[d]Sum of *m/z* 169, 170, 151 (the dehydrated fragment of *m/z* 169), and 152.
[e]A ll yields reported by *Jaoui and Kamens* [2001] are % carbon yields. The yields listed above are converted from % carbon to % total mass yields for comparison with yields obtained from this and other studies.
[f]All yields reported by *Jaoui and Kamens* [2001] are % carbon yields. The yields listed above are converted from % carbon to % total mass yields for comparison with yields obtained from this and other studies.
[g]Yield of α-campholenal (MW = 152).
[h]Yield of norpinonaldehyde (MW = 154).
[i]Sum of norpinonic acid (MW = 170) and pinalic4-acid (MW = 170) yields, with yields of pinalic-4-acid roughly 12 times larger than yields of norpinonic acid.
[j]Sum of pinonic acid (MW = 184) and 1-hydroxypinonaldehyde (MW = 184) yields, with pinonic acid yields roughly 4–8 times larger than 1-hydroxypinonldehyde.
[k]Yield of 4-methyl-3-cyclohexen-1one (MW = 110).
[l]Yield of 4-vinyl-4-pentanal (MW = 110).

as *m/z* 171, 153, and 143. A partial mechanism for the formation of these ions is shown in Figure 6. Other ions are formed even later, such as *m/z* 218, which is likely an organic nitrate compound produced at a low observed yield of <1% (Table 10), and *m/z* 113, which was the dominant ion observed at Blodgett Forest. Molar yields of other unidentified ions totaled 61%, and the carbon mass balance at the end of the experiment was 113 ± 17%, suggesting that the concentrations of unidentified oxidation products to the carbon balance are overestimated and may have resulted from incorrect assignments of carbon number to the product ions or from overestimating the %C in the SOA formed.

3.2.2. Myrcene

[27] The photooxidation of myrcene, an acyclic terpene, produced relatively high yields of SOA (43%) compared to other monoterpenes, in contrast to the low yields (~12%) obtained from myrcene ozonolysis [*Lee et al.*, 2006]. The lifetimes of myrcene with respect to 50 ppb O_3 or 2×10^6 molecules OH cm^{-3} are similar (28 minutes and 39 minutes, respectively), suggesting that ozonolysis and photooxida-

Table 9c. Comparison of Gas-Phase Oxidation Product Yields From Monoterpenes, on a Percent Mole (ppb/ppb) Basis, Observed in This Study With Results From Other Terpene Photooxidation Experiments

Terpene	Product	Product Yield, % This Work	Product Yield, % Other Studies	Reference
β-pinene	formaldehyde	49	54	[*Hatakeyama et al.*, 1991]
			45 ± 8	[*Orlando et al.*, 2000]
			23 ± 2	[*Larsen et al.*, 2001]
			31[a]	[*Librando and Tringali*, 2005]
			30.3	[*Jaoui and Kamens*, 2003b]
	formic acid	8.2	38 ± 4[a]	[*Larsen et al.*, 2001]
			5[a]	[*Librando and Tringali*, 2005]
			2 ± 1	[*Orlando et al.*, 2000]
	acetone	7.9	16 ± 2	[*Wisthaler et al.*, 2001]
			11 ± 3[a]	[*Larsen et al.*, 2001]
			8.5 ± 2	[*Aschmann et al.*, 1998]
			6.5	[*Jaoui and Kamens*, 2003b]
			2 ± 2	[*Orlando et al.*, 2000]
	nopinone	17	79 ± 8	[*Hatakeyama et al.*, 1991]
			27 ± 4	[*Hakola et al.*, 1994]
			30 ± 5	[*Arey et al.*, 1990]
			25 ± 5[a]	[*Larsen et al.*, 2001]
			25 ± 3	[*Wisthaler et al.*, 2001]
			15.2	[*Jaoui and Kamens*, 2003b]
	m/*z* 151	1.4 ± 0.3	0.9	[*Jaoui and Kamens*, 2003b]
	m/*z* 153	2.8 ± 0.6	1.9[b]	[*Jaoui and Kamens*, 2003b]
	m/*z* 155	0.8 ± 0.2	5.3[c]	[*Jaoui and Kamens*, 2003b]
	m/*z* 171	0.1 ± 0.03	<0.1[d]	[*Jaoui and Kamens*, 2003b]
	m/*z* 185	0.1 ± 0.02	0.5[e]	[*Jaoui and Kamens*, 2003b]
γ-terpinene	acetone	5	10 ± 3	[*Reissell et al.*, 1999]
α-terpinene	acetone	3	∼10	[*Reissell et al.*, 1999]

[a]From experiments where the photolysis of H_2O_2 was used as the OH source.
[b]Sum of yields of β-pinene oxide (1%) and 3-oxonopinone (0.9%). A trace amount of myrtenol was reported but not quantified and is not included in the sum.
[c]Sum of yields of 1-hydroxynopinone (3.1%) and 3-hydroxynopinone (2.2%).
[d]Yield of 3,7-dihydroxynopinone.
[e]Yield of pinonic acid.

tion are both important loss processes in the real atmosphere. High yields of formaldehyde (74%) and acetone (22%), and low yields of formic and acetic acid (<5%) were observed. Our yield of acetone is slightly lower than the 36% reported by *Orlando et al.* [2000] and the 41% yield reported by *Reissell et al.* [1999]. While our yield of formic acid is the same as the yield obtained elsewhere [*Orlando et al.*, 2000], our yield of formaldehyde is much higher than the 30% yield of *Orlando et al.* [2000]. Because the formaldehyde mixing ratios in the chamber (∼110 ppb) were beyond the range of the calibrated linear response, the formaldehyde yield from myrcene is subject to considerable error.

[28] Numerous compounds can be produced from myrcene due to the many possible sites for OH attack. Many product ions were detected, with highest molar yields from *m*/*z* 93 (32 ± 6.8%) and 113 (32 ± 6.7%). The product 4-vinyl-4-pentenal (MW = 110) was identified from other studies [*Reissell et al.*, 2002], and was observed from myrcene ozonolysis at *m*/*z* 111 and 93 [*Lee et al.*, 2006]. However, from these photooxidation studies, *m*/*z* 111 and 93 were not well correlated (R^2 = 0.5) and exhibited different loss rates with time (Figure 7) where *m*/*z* 93 was oxidized completely, as expected given that 2 two double bonds remain in the structure, whereas *m*/*z* 111 was not, suggesting that other compounds likely interfered on *m*/*z* 111. Additionally, *m*/*z* 111 correlated well with other ions, e.g., *m*/*z* 71 (R^2 = 0.96), 83 (R^2 = 0.97), 97, 113, and 139 (all R^2 = 0.93). These correlations were not observed from the ozonolysis studies [*Lee et al.*, 2006], and may indicate that these ions are fragments of the same compound, or that these ions represent different compounds that are produced and consumed at similar rates. 4-vinyl-4-pentenal is likely detected at both *m*/*z* 111 and 93, but another product or

Table 10. Yields of Organic Nitrate Oxidation Products[a]

Terpene	*m*/*z*	Yield, %
longifolene	220	0.8 ± 0.2
limonene	200	0.1 ± 0.02
	218	0.2 ± 0.04
myrcene	64	0.1 ± 0.03
methyl chavicol	124	0.4 ± 0.1
	168	0.5 ± 0.1
	170	0.3 ± 0.1
	180	0.5 ± 0.1
	182	0.1 ± 0.03
α-pinene	94	0.9 ± 0.2
	200	0.2 ± 0.04
β-pinene	108	1.9 ± 0.4
	184	0.1 ± 0.05
	198	0.2 ± 0.04
γ-terpinene	230	0.1 ± 0.02
α-terpinene	178	0.05 ± 0.02
	184	0.1 ± 0.05
	202	0.1 ± 0.03
	230	0.2 ± 0.04
verbenone	230	0.1 ± 0.02
linalool	188	0.2 ± 0.05

[a]Reported yields are limited to those oxidation products with even mass-to-charge ratios that are unambiguously not carbon isotopes of the preceding *m*/*z*.

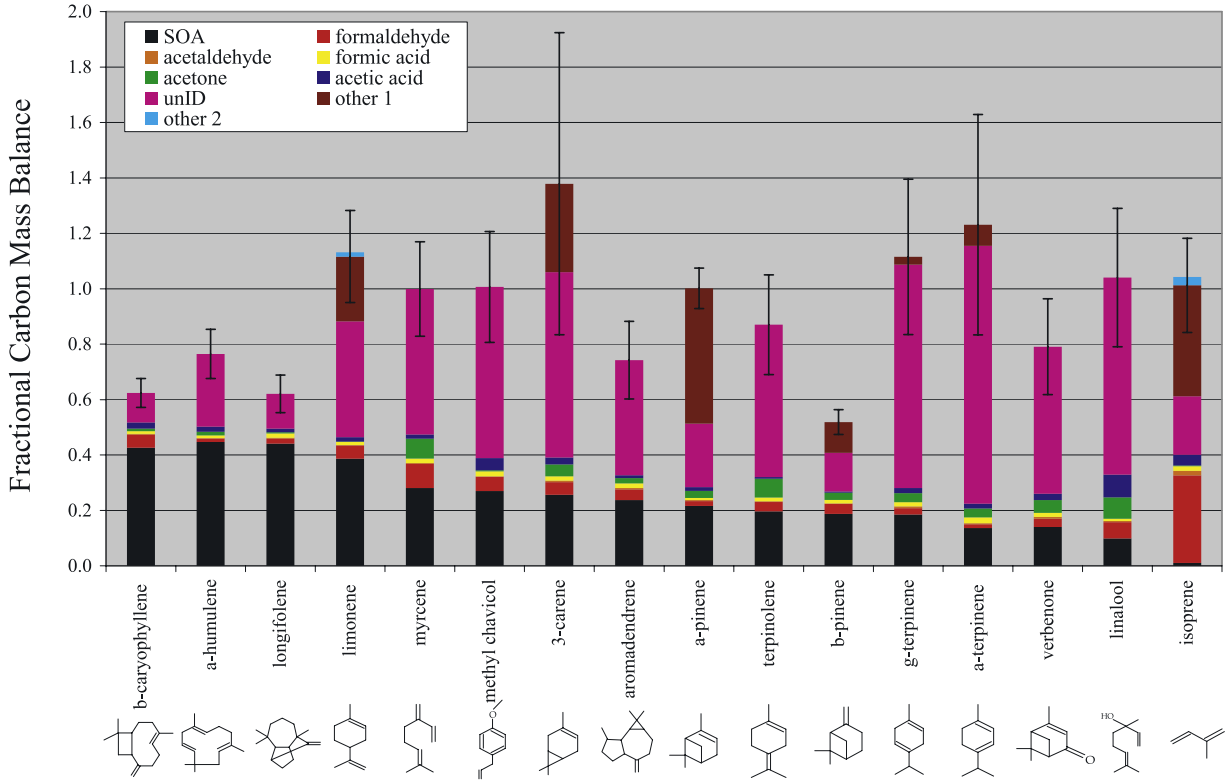

Figure 2. Carbon mass balance of SOA (assuming aerosol is 60% carbon) and gas-phase oxidation products, represented as a 30–60 minute snapshot in time at the middle or end of the experiment for the purpose of carbon accounting, and does not represent overall stoichiometric yields. The "other 1" category represents the calibrated products nopinone and MACR + MVK from β-pinene and isoprene, respectively, and the uncalibrated products limononaldehyde, caronaldehyde, pinonaldehyde, γ-terpinaldehyde, and α-terpinaldehyde, from limonene, 3-carene, α-pinene, γ-terpinene, and α-terpinene, respectively. The "other 2" category represents limonaketone from limonene and 3-methyl furan from isoprene. Aerosol molar yields (μg aerosol m^{-3}/μg terpene m^{-3}) were calculated assuming an aerosol density of 1.25 g cm^{-3}.

products might interfere on *m*/*z* 111. Thus, our reported yield of 4-vinyl-4-pentenal of 41% (Table 9a) is likely overestimated, but by no more than 9%. The total gas-phase carbon balance for myrcene was 100 ± 17%.

[29] Figure 7 shows the time series plots for selected ions. Acetone and the compounds occurring on *m*/*z* 71, 93, 111, 113, and 139 are clearly first-generation oxidation products, as their concentrations peak as myrcene becomes completely oxidized. All of these compounds decreased in concentration after myrcene was fully consumed. In contrast, the product occurring on *m*/*z* 115 was clearly a second-generation product, as its concentration continued to increase after complete consumption of myrcene. Figure 8 shows potential structures for some of the ions shown in Figure 7. The production of *m*/*z* 113 from myrcene photooxidation as a first-generation product, and at a high molar yield, is surprising because it was formed as a second-generation product in myrcene ozonolysis [*Lee et al.*, 2006], suggesting that different products from photooxidation and ozonolysis contribute to observations of *m*/*z* 113 in ambient air. A product with *m*/*z* 113 can be formed simply from oxidation of 4-vinyl-4-pentenal (*m*/*z* 111), as suggested for myrcene ozonolysis [*Lee et al.*, 2006], however, as shown in Figure 8, production of *m*/*z* 113 as a first-generation product directly from myrcene photooxidation is more complicated and may involve the co-production of a compound with *m*/*z* 89 and a dehydrated fragment of *m*/*z* 71. A possible alternative to the exotic cyclization step shown in Figure 8 is the formation of the acyclic tricarbonyl species by internal rearrangement of a peroxy radical [*Vereecken and Peeters*, 2004], which may oxidize multiple double bonds in a single oxidation step. Myrcene photooxidation was the dominant source of *m*/*z* 113 observed from all photooxidation and ozonolysis experiments.

3.2.3. 3-Carene, α-Pinene, and β-Pinene

[30] Compared to the other terpenes discussed here, 3-carene, α-pinene and β-pinene have been relatively well studied, and thus, we will not present a detailed discussion of the photooxidation of these compounds. SOA yields obtained here from 3-carene photooxidation (38%) are higher than those obtained elsewhere [*Hoffmann et al.*, 1997] and [*Griffin et al.*, 1999], which is generally consistent with the lower temperature of our experiment. From 3-carene ozonolysis, SOA yields (54%) were higher than from photooxidation. Our formaldehyde yield was higher than those observed elsewhere, and yields of formic acid and acetone were lower than other studies (Table 9a), but the sum of all caronaldehyde-associated ions (Table 3a)

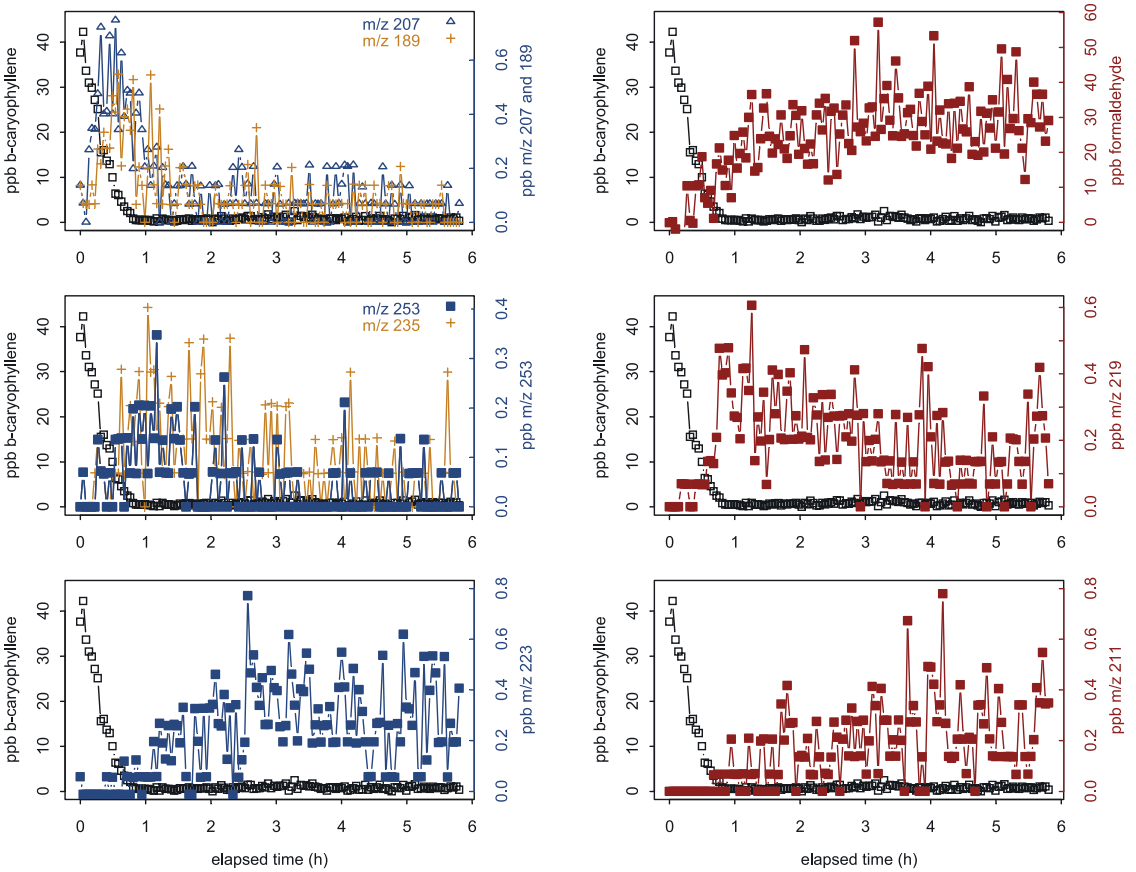

Figure 3. Photooxidation of β-caryophyllene shows the production of primary (m/z 207, 189), secondary (m/z 253, 235, 219), and perhaps delayed secondary or tertiary (m/z 223, 211) oxidation products.

produced much higher yield (77%) than yields observed from other studies (Table 9a). In contrast, caronaldehyde was produced at very low yields from the ozonolysis of 3-carene (<1%). The high SOA yield and low caronaldehyde yields from 3-carene ozonolysis, and the lower SOA yield and higher caronaldehyde yield from 3-carene photooxidation suggest that caronaldehyde does not readily partition into the particle phase. Caronaldehyde was not calibrated in the PTR-MS, and the calculated yield of this product is based on the sum of all ions (Table 3a) that are well correlated with *m/z* 169 and 151, the dominant caronaldehyde ions. The very high yield of caronaldehyde observed from these photooxidation experiments compared to other work may suggest that this correlation method overestimates caronaldehyde yields by incorrectly attributing certain ions to caronaldehyde. This method was also used for pinonaldehyde from α-pinene, which agreed well with many of the previous experiments when only *m/z* 151, 152, 169, and 170 were accounted for, but was within the higher range of other results when all ions that correlated well with *m/z* 151 and 169 were included (Table 9b). The yield of limononaldehyde from limonene was also higher than previous results, further suggesting that some of the ions we found to be correlated with *m/z* 151 and 169 from the keto-aldehyde produced from attack at the internal double bond, and were reported as fragments from a pinonaldehyde standard by [*Wisthaler et al.*, 2001] may not be fragments of the keto-aldehyde, or, more likely, may suffer from interference from other compounds.

[31] SOA yield from α-pinene photooxidation agrees relatively well with other studies [*Noziere et al.*, 1999] and [*Jaoui and Kamens*, 2001]. Compared to other terpenes, α-pinene was not a significant source of the low molecular weight products (Table 6) and yields of these products are slightly lower than those observed elsewhere (Table 9b). Our pinonaldehyde yield is generally higher, but within the range of those observed elsewhere. A theoretical study was conducted on the OH oxidation of α-pinene and predicted higher yields of pinonaldehyde (∼60% versus ∼36%) under lower NO (normal atmospheric conditions) compared to the higher NO conditions of many laboratory chamber experiments [*Peeters et al.*, 2001].

[32] SOA yield from β-pinene was 31%, similar to the yield obtained by *Hoffmann et al.* [1997] and *Griffin et al.* [1999], obtained under a lower HC:NO_x ratio and higher temperatures, and was higher than the 21% SOA yield obtained by *Jaoui and Kamens* [2003b] under a similar HC:NO_x ratio and slightly higher temperatures (Table 5). The observed yields of formaldehyde, formic acid, and acetone (Table 9c) were similar to those observed elsewhere [*Hatakeyama et al.*, 1991; *Orlando et al.*, 2000; *Jaoui and Kamens*, 2003b; *Aschmann et al.*, 1998]. However, *Larsen et al.* [2001] observed a lower yield of formaldehyde, and significantly higher yields of formic acid in experiments

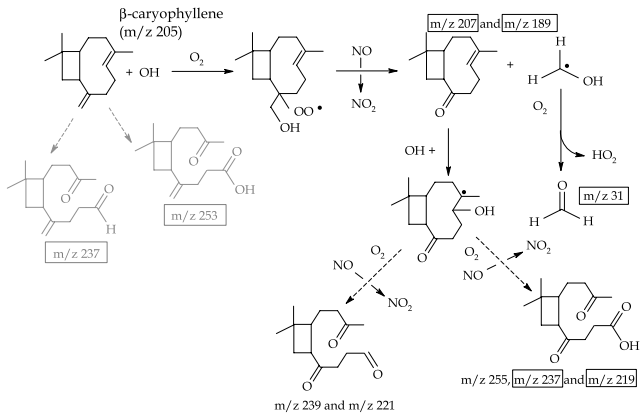

Figure 4. Partial mechanisms for β-caryophyllene photooxidation. The boxed product ions represent observed ions, and the gray structures were products observed from β-caryophyllene ozonolysis, but were not observed by PTR-MS as gas-phase photooxidation products.

conducted under low NO_x levels, which is suggestive of the favored production of formic acid over formaldehyde after OH addition to the terminal carbon of the exo double bond under low NO_x.

[33] Nopinone has been reported to be the dominant product from the ozonolysis and photooxidation of β-pinene, and our observed photooxidation yield of 17% is comparable to the 15.2% yield reported by *Jaoui and Kamens* [2003b], but low compared to most other studies, which range from 25–27%, with a highest reported yield of 79% (Table 9c). Numerous other products have been reported, including β-pinene oxide, oxonopinone, hydroxynopinones, and pinonic acid [*Jaoui and Kamens*, 2003b]. Our yields of ions corresponding with previously reported products are comparatively low for the hydroxynopinones and pinonic acid, but high for the sum of β-pinene oxide and 3-oxonopinone (*m/z* 153). Our low carbon mass balance of 52 ± 5% from β-pinene photooxidation suggests that yields of nopinone, or other high molecular weight oxidation products, were underestimated, or not detected.

3.2.4. Terpinolene

[34] Terpinolene photooxidation produced an SOA yield of 31% and high molar gas-phase yields (43%) of the oxidation product ions at *m/z* 111 and 93, the dehydrated fragment of 111 ($R^2 = 0.96$), corresponding to the identified product 4-methyl-3-cyclohexen-1-one [*Hakola et al.*, 1994] produced from primary OH attack at the exocyclic double bond. Our observed yield of 4-methyl-3-cyclohexen-1-one is higher than reported elsewhere, whereas we observed very little production of *m/z* 169 (0.5%), the C_{10} ketoaldehyde formed from OH attack at the endocyclic double bond, which has been observed at a 10% yield elsewhere [*Arey et al.*, 1990]. Our measured yields of formaldehyde (23%), formic acid (4%), and acetone (20%) are lower than yields reported elsewhere of ~30%, 8%, and ~40%, respectively (Table 9b). The yield of *m/z* 111 + 93 was

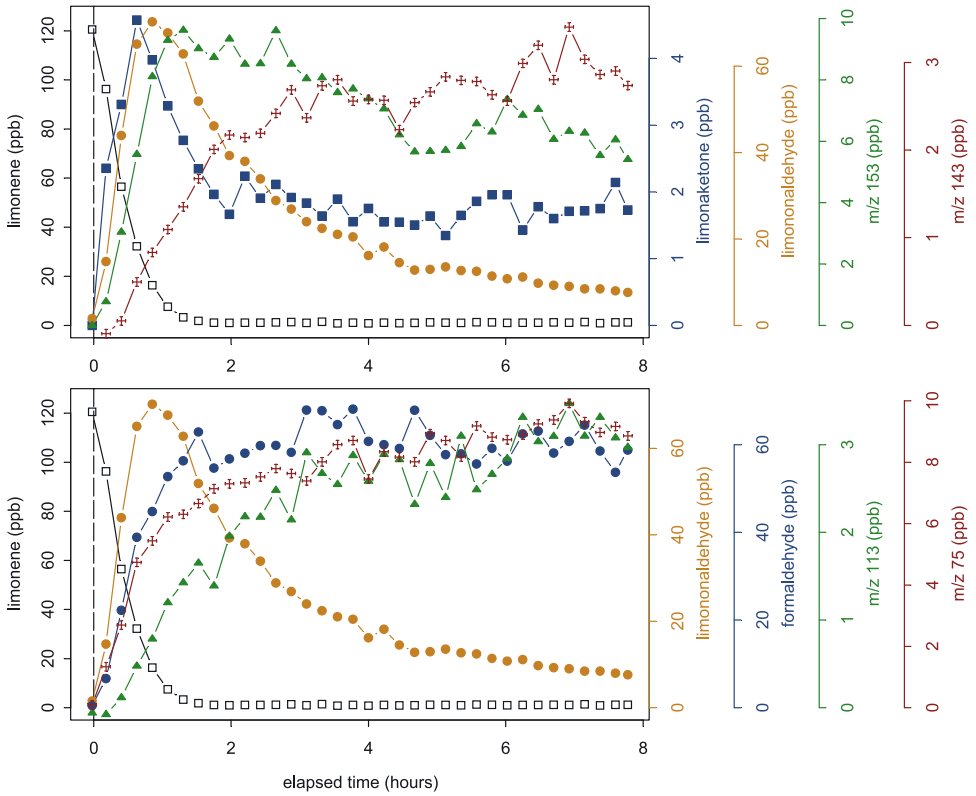

Figure 5. Time series of selected products from limonene photooxidation. Blue squares represent limonaketone (top) or formaldehyde (bottom). Orange circles represent limononaldehyde (top and bottom). Green triangles represent *m/z* 153 (top) or 113 (bottom). Red crosses represent *m/z* 143 (top) or 75 (bottom).

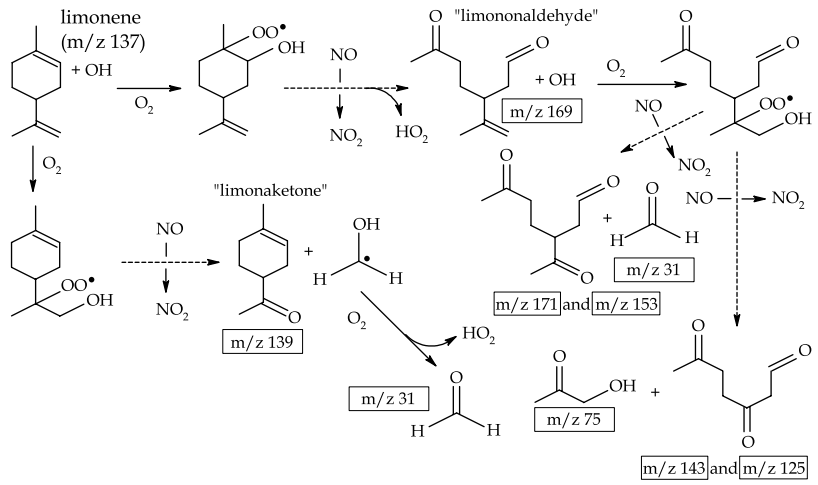

Figure 6. Partial mechanisms for the production of selected product ions from limonene photooxidation. Because we focus on major product ions, or product ions that were also observed by in ambient air by *Holzinger et al.* [2005], for clarity, other likely pathways and products are not shown.

dominant, but significant production of *m/z* 87, 99, 143 (6%, 16%, and 5%, respectively) was observed as well. *m/z* 113 was also produced, with a yield of ~3%.

[35] The time series of terpinolene photooxidation (Figure 9) shows that 4-methyl-3-cyclohexen-1-one and acetone were formed quickly by OH addition to the exocyclic double bond (Figure 10). The further oxidation of

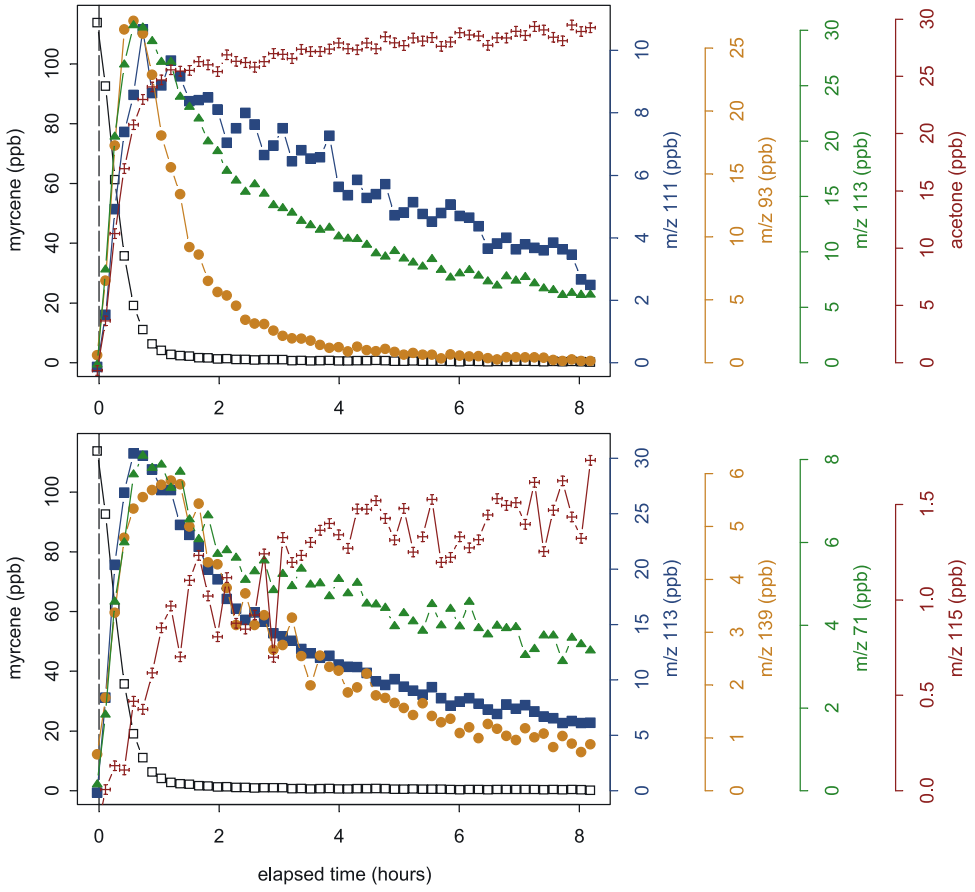

Figure 7. Time series of selected products from myrcene photooxidation. Blue squares represent *m/z* 111 (top) or 113 (bottom). Orange circles represent *m/z* 93 (top) or 139 (bottom). Green triangles represent *m/z* 113 (top) or 71 (bottom). Red crosses represent acetone (top) or *m/z* 115 (bottom).

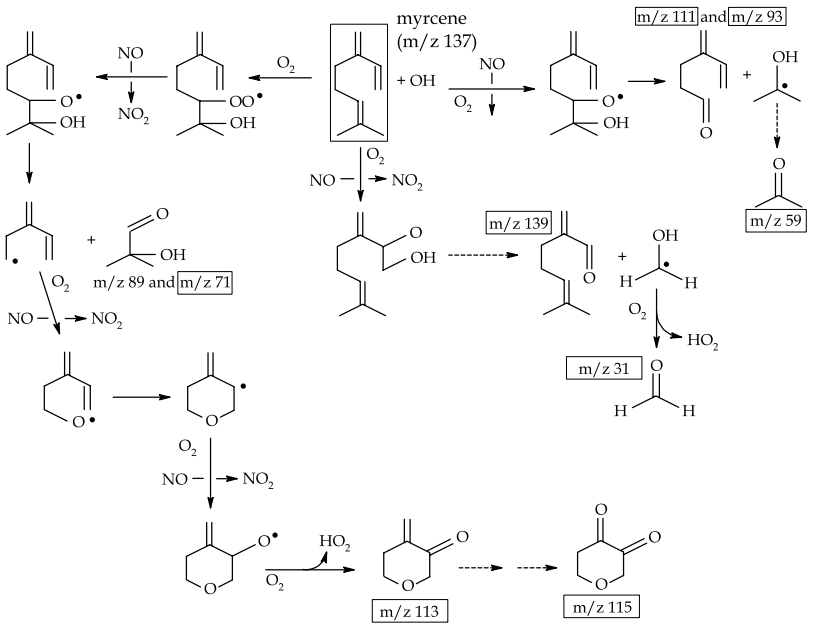

Figure 8. Partial mechanisms for the production of selected ions from myrcene photooxidation. Because we focus on major product ions, or the product ions that were also observed by in ambient air by *Holzinger et al.* [2005], for clarity, other likely pathways and products are not shown. Note that the compounds occurring on *m*/*z* 113 and 115 can be produced as second and third-generation products from the further oxidation of *m*/*z* 111, however, the time series data (Figure 7) clearly show that *m*/*z* 113 is produced as a first-generation product. A possible alternative to the exotic cyclization step shown is the formation of the acyclic tricarbonyl species by internal rearrangement of a peroxy radical [*Vereecken and Peeters*, 2004], which may oxidize multiple double bonds in a single oxidation step.

4-methyl-3-cyclohexen-1-one at the remaining internal double bond was also rapid, and likely led to the production of *m*/*z* 143 (a C_7 keto-keto-aldehyde), 99, and 113. The C_7 keto-keto-aldehyde (*m*/*z* 143) was oxidized further (Figure 9) and likely led to the production of other product ions, including *m*/*z* 115 (Figure 10). Numerous other reaction pathways and products are likely to be formed from oxidation of *m*/*z* 143, however, for simplicity, only one pathway, leading to the production of *m*/*z* 115, is shown in Figure 10. Hydrogen abstraction from 4-methyl-3-cyclohexen-1-one (*m*/*z* 111) by OH can also lead to the production of a compound with *m*/*z* 113 (Figure 10), which was observed as a second-generation product (Figure 9).

[36] Terpinolene has been observed in ambient air at Blodgett Forest, but does not represent a dominant monoterpene measured above the canopy [*Lee et al.*, 2005]. However, its shorter lifetime with respect to O_3 compared to OH oxidation, and the relatively high yields of *m*/*z* 111 and 113, suggest that terpinolene may contribute to the chemical O_3 deposition [*Kurpius and Goldstein*, 2003] and high in-canopy mixing ratios of *m*/*z* 111 and 113 observed at Blodgett Forest [*Holzinger et al.*, 2005].

3.2.5. γ-Terpinene

[37] Yields of SOA, as well as yields of the calibrated low molecular weight oxidation products from γ-terpinene are low compared to other monoterpenes. In contrast, the molar yield (ppb product/ppb terpene) of *m*/*z* 169 and the ions associated with this C_{10} keto-aldehyde (γ-terpinaldehyde), of which there are two possible isomers resulting from the oxidation of either double bond, was 57 ± 6%, and the molar yield of all product ions (excluding those associated with γ-terpinaldehyde) was 130 ± 10%, suggesting that many other unidentified products are formed from γ-terpinene. γ-terpinaldehyde was formed quickly as a first-generation oxidation product and upon further oxidation of either isomer of *m*/*z* 169, *m*/*z* 69 + 87 and 115 would also be formed quickly. Other oxidation products are formed as second-generation products, including *m*/*z* 103 + 85, 131 + 113, and 101. Oxidation of γ-terpinene by 2×10^6 molecules OH cm^{-3} is faster than by 50 ppb O_3 (47 minutes versus 95 minutes), suggesting that OH oxidation of γ-terpinene in the real atmosphere likely dominates, and contributes to the observations of *m*/*z* 123, 151, and 169 in ambient air (Table 7).

3.2.6. α-Terpinene

[38] Like γ-terpinene, yields of SOA and low molecular weight products from α-terpinene are low. The photooxidation of α-terpinene was rapid and α-terpinaldehyde, with two possible isomers at *m*/*z* 169 (Table 3b), *m*/*z* 125, 157 + 139, and 185 + 167 were the first products observed, and thus appear to be first-generation products. However, these ions do increase in concentration after complete consumption of α-terpinene, suggesting that multiple products occur on these masses, or that these ions are not first-generation products. Other ions are clearly formed as second-generation products, including formaldehyde, acetone, and *m*/*z* 99, 115, and 143. Yields of α-terpinaldehyde (19 ± 2%) and *m*/*z* 143 (13 ± 3%) were dominant. Excluding the ions associated with α-terpinaldehyde, the molar yield of unidentified products was ~60%, suggesting that many other important

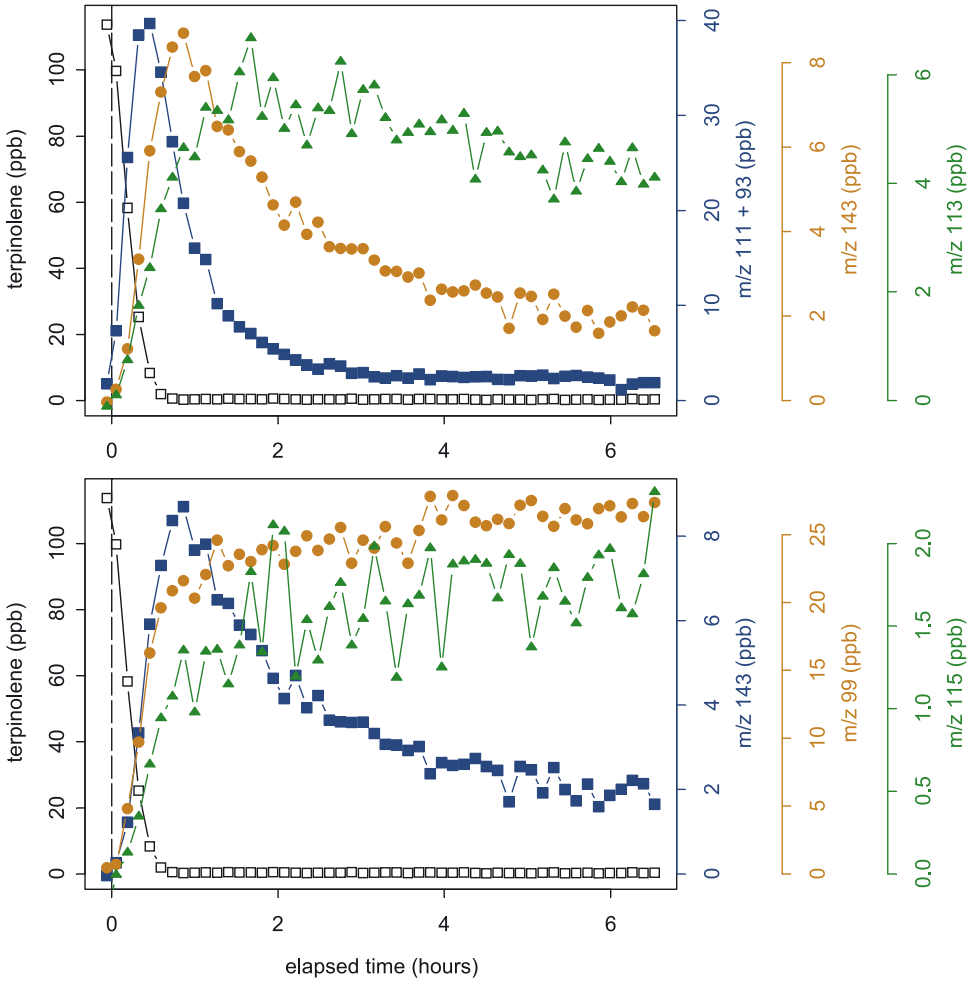

Figure 9. Time series of selected products from terpinolene photooxidation. Blue squares represent *m/z* 111 + 93 (top) or 143 (bottom). Orange circles represent *m/z* 143 (top) or 99 (bottom). Green triangles represent *m/z* 113 (top) or 115 (bottom).

products were formed, including four potential organic nitrate products occurring at *m/z* 178, 184, 202, and 230 (Table 10). Despite the rapid oxidation of α-terpinene and the uncertainty over observing first-generation products, the carbon mass balance was 123 ± 40%, suggesting we have overestimated the %C in the SOA formed or the amount of gas-phase products observed.

3.3. Oxygenated Terpenes and Isoprene

3.3.1. Methyl Chavicol

[39] SOA yield from methyl chavicol was highest of all oxygenated terpenes (40%), and also considerably higher than the SOA yield obtained from methyl chavicol ozonolysis [*Lee et al.*, 2006]. High yields of formaldehyde (52 ± 6%) were also observed, as expected due to its external double bond, and acetic acid was also produced at high yield (25 ± 2%). OH addition to the terminal carbon of the external double bond can result in the formation of an aldehyde with *m/z* 151 ($C_9H_{10}O_2$) plus formaldehyde, or an aldehyde with *m/z* 137 ($C_8H_8O_2$) plus glycolaldehyde (hydroxyl acetaldehyde), with *m/z* 61. The observations of *m/z* 61 were likely glycolaldehyde, not acetic acid. The C_9 compound on *m/z* 151 was observed at a yield of 23 ± 5%, while the C_8 compound on *m/z* 137 was produced at a yield of 42 ± 9%. All of these dominant ions were first-generation products. Glycolaldehyde was not calibrated in the PTR-MS, however, calculation of glycolaldehyde yield can be approximated by the sum of *m/z* 61 and 43, or from the calibration of acetic acid, assuming they behave similarly in the PTR-MS. The sum of yields of *m/z* 61 + 43 was 37 ± 5%, higher than the 25% yield using the acetic acid calibration factor. The higher yield is in better agreement as a co-product of *m/z* 137. The yield of formaldehyde is ~20% higher than the yield of *m/z* 151, suggesting that the compound occurring at *m/z* 151 may be underestimated due to fragmentation. Five potential organic nitrate compounds were also produced at low observed yields of <1% (Table 10).

3.3.2. Verbenone

[40] SOA yield from verbenone, and oxygenated terpene with a similar structure to α-pinene, was low (19%). A high yield of formaldehyde (32%) was observed, which was not expected, given its endo double bond. Numerous oxidation product ions were observed, but yields were generally low

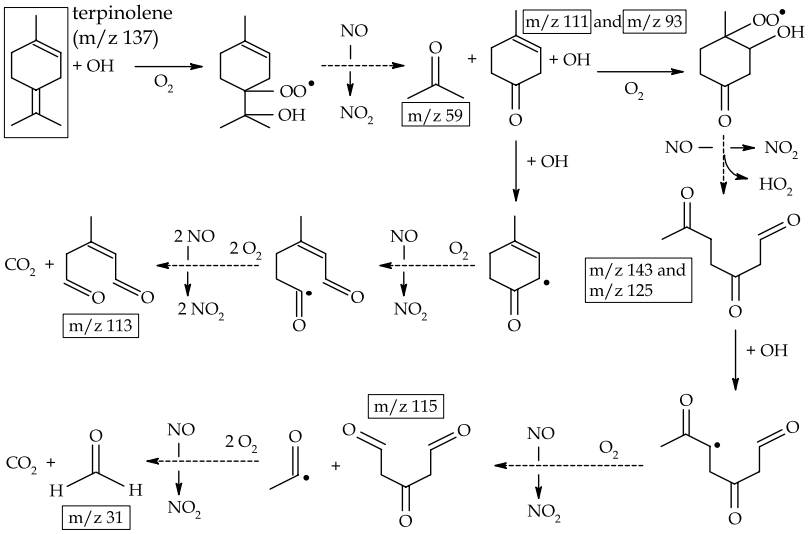

Figure 10. Partial mechanisms for the production of selected ions from terpinolene photooxidation. Because we focus on major product ions, or the product ions that were also observed by in ambient air by *Holzinger et al.* [2005], for clarity, other likely pathways and products are not shown.

for all ions, with the highest yield observed on *m*/*z* 71, at 12 ± 3%. The carbon mass balance (79 ± 17%) was low compared to other C_{10} terpenes, suggesting that product ions were underestimated, possibly due to losses in tubing.

3.3.3. Linalool

[41] Linalool photooxidation produced SOA in substantially higher yield (13%) than from ozonolysis (1%) [*Lee et al.*, 2006]. As expected from its structure, linalool produced high yields of formaldehyde (43%) and acetone (25%). Numerous other product ions were observed. The dominant product was the C_7 compound, formed with acetone from OH attack on the internal double bond, occurring on *m*/*z* 129 and its dehydrated fragments *m*/*z* 111 (R^2 = 0.97) and 93 (R^2 = 0.98), formed at a yield of 75 ± 10%. A product with MW = 128 has been reported elsewhere as 4-hydroxy-4-methyl-5-hexen-1-al and its cyclized isomer, with a yield of 46% [*Shu et al.*, 1997], which is nearly 1.6 times smaller than our observed yield (Table 8). OH attack at the internal double bond is expected to dominate over addition to the terminal double bond with a ratio of ~77%/23% [*Shu et al.*, 1997]. This ratio is roughly consistent with our 75% yield of 4-hydroxy-4-methyl-5-hexen-1-al, but inconsistent with the 46% yield observed by [*Shu et al.*, 1997]. The formation of this product should also lead to the co-production of acetone, however, our low acetone yield, which is also low compared to the 51% reported elsewhere [*Shu et al.*, 1997], suggests that our acetone yield may be underestimated. Alternatively, our yield of 4-hydroxy-4-methyl-5-hexen-1-al may also be overestimated as a result of interference of other compounds on *m*/*z* 93, 111, or 129. Because of the good correlations between *m*/*z* 93 and 111 with *m*/*z* 129, and because of the good agreement in our 75% yield of the product formed from OH attack at the internal double bond with the expected branching ratio reported by [*Shu et al.*, 1997], we believe that our yield of 4-hydroxy-4-methyl-5-hexen-1-al is reasonable, but cannot find an explanation for the low yields we observed of the acetone co-product. *Shu et al.* [1997] also observed that OH attack at the terminal double bond produces 6-methyl-5-hepten-2-one ($C_8H_{14}O$, MW = 126), with a yield of 6.8%, with the co-production of glycolaldehyde ($C_2H_4O_2$, MW = 60), which was not observed by *Shu et al.* [1997]. We observed a comparable yield of 8% for *m*/*z* 127, and yield of 17% for *m*/*z* 61, which may be dominated by glycolaldehyde but may still include some contribution from acetic acid. Numerous ions produced at high yields were observed in addition to the dominant C_7 product, including *m*/*z* 75, 99, 101, and 127, and were produced as different generational products, suggesting that the photooxidation of linalool results in numerous different products formed through a variety of mechanistic pathways. The carbon balance for linalool was 104 ± 25%.

3.3.4. Isoprene

[42] SOA yield from isoprene photooxidation was low (2%), as has been shown from previous studies [*Pandis et al.*, 1991; *Kroll et al.*, 2005]. A high molar yield of formaldehyde (160%) contributed to <30% of the total carbon. The yields of methacrolein (MACR) and methyl vinyl ketone (MVK) could not be differentiated because they occur on the same *m*/*z*, thus we report the sum of the two products, whose yield ranged from 60–87 ± 11%. The reported range results from uncertainty in the use of individual calibration factors for MACR and MVK in obtaining a concentration of the sum of the two compounds. The lower yield of MACR + MVK was calculated from a calibration factor that was the weighted average of individual calibrations factors for MVK:MACR of 1.45:1, based on reported yields of MVK and MACR from previous studies [*Atkinson and Arey*, 2003] and references therein. The higher yield of MACR + MVK was calculated from a calibration factor from a cylinder standard containing a mix of MVK and MACR in a ratio of 1.04:1 (MVK:MACR). Our observed yields of MACR + MVK were higher, but near the range of those obtained previously (Table 8). The yield of formaldehyde from isoprene oxidation that we obtained was extremely high compared to other studies.

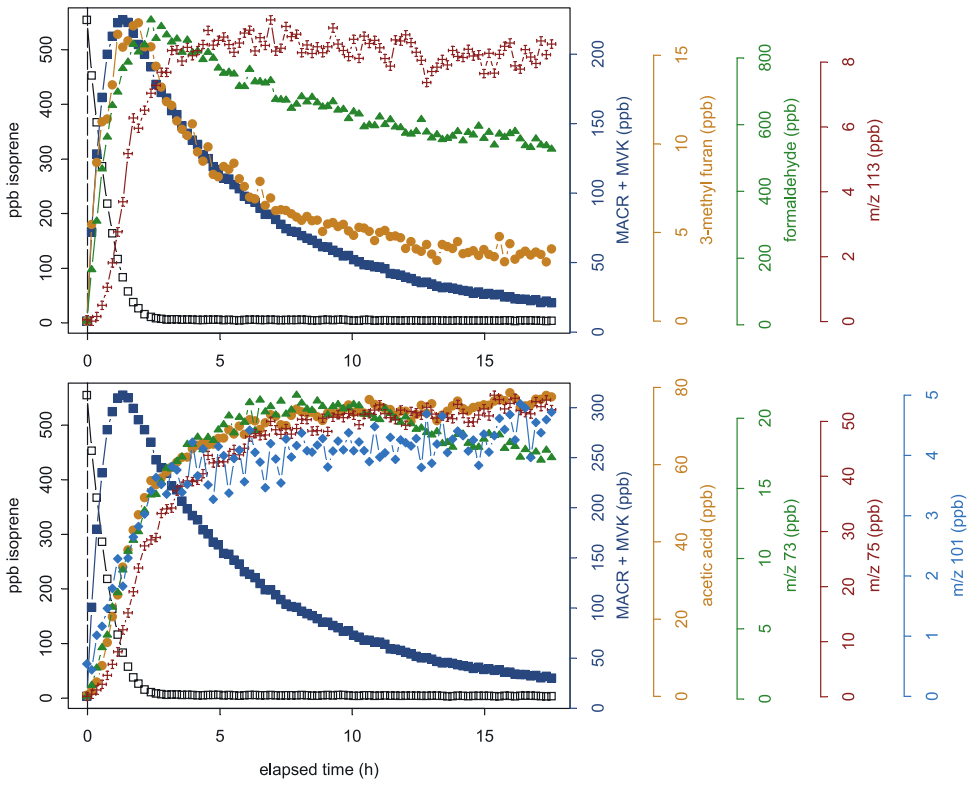

Figure 11. Time series of selected products from isoprene photooxidation. Blue squares represent MACR + MVK (top and bottom). Orange circles represent 3-methylfuran (top) or acetic acid (*m*/*z* 61) (bottom). Green triangles represent formaldehyde (top) or *m*/*z* 73 (bottom). Red crosses represent *m*/*z* 113 (top) or *m*/*z* 75 (bottom). The light blue diamonds represent *m*/*z* 101 (bottom).

Because the starting concentration of isoprene was high (~500 ppb), mixing ratios of formaldehyde were also high and well beyond the range of the calibrated linear response. Thus, the formaldehyde yield from isoprene is subject to significant error.

[43] Previously reported yields of MACR + MVK range from 54–61%, which is similar to our yield based on the weighted average of individual MACR and MVK calibration factors, suggesting that for isoprene oxidation, the PTR-MS is sensitive to the identities of the products that occur on *m*/*z* 71. In contrast to the high yields observed for formaldehyde and MACR + MVK, our yield of 3-methyl furan is similar to those reported elsewhere (Table 8). The carbon balance for isoprene was 101–114 ± 22%. Other products identified by their *m*/*z*, including *m*/*z* 73, 75, 85, 99, 101 and 113, contributed to 20% of the carbon during the period when MACR + MVK and formaldehyde were co-dominant (~2.5–3 hours).

[44] The time series for isoprene oxidation product ions show that several products are first-generation, including MACR + MVK and 3-methyl furan, and other products are second-generation, including *m*/*z* 113, and the ions *m*/*z* 61, 73, and 75 (Figure 11). The observed signal on *m*/*z* 61, reported as acetic acid (~6% yield), may result from the production of glycolaldehyde, and *m*/*z* 73 and 75, likely corresponding to methylglyoxal and hydroxyacetone. Several ions were observed from isoprene photooxidation, including *m*/*z* 113, a dominant ion observed in ambient air [*Holzinger et al.*, 2005], and *m*/*z* 101 (Table 8), which has also been observed by PTR-MS in ambient air above a tropical rain forest [*Warneke et al.*, 2001] and a tropical savanna [*Holzinger et al.*, 2002], and may be the C_5 hydroxycarbonyls reported by *Zhao et al.* [2004] and *Baker et al.* [2005].

[45] The production of hydroxycarbonyls from OH oxidation of isoprene were reported by *Kwok et al.* [1995], but were not quantified due to the lack of standards for those compounds. Using PTR-MS, *Zhao et al.* [2004] reported yields of C_5 hydroxycarbonyl products, based on the detection of *m*/*z* 101, of 19 ± 6%, similar to the estimated combined yield of ~15% of two C_5 hydroxycarbonyls [*Baker et al.*, 2005]. These two yields are much larger than our observations of *m*/*z* 101 (Table 8). If *m*/*z* 101 is indeed a C_5 hydroxycarbonyl, we expect the compound to dehydrate and produce a fragment at *m*/*z* 83, and possibly *m*/*z* 65. The dominant ion produced from 3-methyl furan, however, also occurs on *m*/*z* 83, thus production of the C_5 hydroxycarbonyl would likely interfere and overestimate yields of 3-methyl furan. The yield of *m*/*z* 65 was only ~30% of *m*/*z* 101 (R^2 = 0.91). Because our observed yield of 3-methyl furan is similar to those reported elsewhere, and because *m*/*z* 101 and 65 were observed at such low mixing ratios, it is likely that the C_5 hydroxycarbonyls were not well detected by the PTR-MS, due to the production of other unknown fragments besides *m*/*z* 83 or 65. Additionally, *Zhao et al.* [2004] did not report the pressure in the PTR-MS reaction

chamber or the observed fragments of the C_5 hydroxycarbonyls, nor did they report yields of 3-methyl furan, thus it is unclear whether significant fragmentation of *m*/*z* 101 occurred, and whether they attributed their observations of *m*/*z* 83 to the C_5 hydroxycarbonyl instead of 3-methyl furan, or if the yield of the C_5 hydroxycarbonyl is based solely on *m*/*z* 101 and yields of 3-methyl furan are not reported for a different reason.

[46] Many ions, including *m*/*z* 113, 101, 75, 73, and 61 (acetic acid + glycolaldehyde) were clearly observed as second-generation products. Second- (or later-) generation products were found to contribute significantly to the SOA formed in this experiment [*Ng et al.*, 2006], and glycolaldehyde, hydroxyacetone, and methylglyoxal have recently been observed in the gas and particle phases in two forested environments in the United States [*Matsunaga et al.*, 2005]. However, other laboratory experiments have shown that SOA composition analyzed with an aerosol mass spectrometer from isoprene oxidation is very similar to SOA from MACR oxidation [*Kroll et al.*, 2006], and that MVK oxidation does not result in SOA production [*Kroll et al.*, 2005], suggesting that MACR oxidation products contributed to the SOA growth observed from isoprene photooxidation.

3.4. Relevance to Ambient Observations of Product Ions

[47] Observations of *m*/*z* 123, 151, and 169 can result from the oxidation of many different terpenes with endo double bonds, including α-pinene, 3-carene, γ-terpinene, α-terpinene, and limonene (Table 7), suggesting that these ions may not be unique indicators of rapid, within-canopy oxidation reactions, because they are formed from both slow and fast reacting terpenes. The ambient observations of *m*/*z* 111 and 113 suggested formation within the forest canopy from rapid oxidation of reactive terpenes [*Holzinger et al.*, 2005]. From these experiments, *m*/*z* 111 was observed at high yields from myrcene, terpinolene, and linalool. *m*/*z* 113 was observed as a product ion from all 16 terpenes, but was only formed at significant yields, and observed as a first-generation product, from myrcene photooxidation, suggesting that myrcene may be the dominant contributor to production of *m*/*z* 113 in ambient air. If concentrations of OH are elevated inside the canopy, as recently suggested [*Goldstein et al.*, 2004; *Farmer et al.*, 2005], the lifetime of myrcene may decrease enough, relative to the canopy mixing time, to contribute to the rapid chemistry suggested by *Holzinger et al.* [2005]. The better carbon mass balance obtained from the C_5 and C_{10} experiments compared to the C_{15} experiments suggest that additional uncertainty exists in the detection and quantification of sesquiterpene oxidation products. Additionally, the reactivity of β-caryophyllene and α-humulene with O_3, and the resulting difficulty in measuring their emission rates, suggest that these compounds or similar compounds are likely important for SOA production and rapid-within canopy chemistry, but their emissions are still poorly characterized and require further study. The results from these photooxidation experiments, and previous ozonolysis experiments [*Lee et al.*, 2006] confirm that the ions observed by *Holzinger et al.* [2005] are consistent with terpene oxidation products. Although the identities of these products and their precursor terpenes remain uncertain, these experiments aid in identifying the important ions that can serve as markers for terpene reactivity and resulting SOA production in the real atmosphere.

4. Conclusions

[48] We conducted photooxidation experiments on 16 different terpenes to measure the time evolution and yields of gas-phase oxidation products and secondary organic aerosol. Yields of formaldehyde, acetone, and a few higher molecular weight oxidation products, such as nopinone, pinonaldehyde, and related acids, have been reported in the literature for a limited number of terpenes, and generally are in good agreement with the yields obtained from our experiments. Yields of SOA are also in good agreement with those reported elsewhere from experiments under similar experimental conditions. In addition to yields of previously reported compounds, we report yields of formaldehyde, acetaldehyde, formic acid, acetone, acetic acid, nopinone, pinonaldehyde, MACR + MVK, and numerous other identified and unidentified compounds characterized by their mass to charge ratio, for the entire suite of 16 terpene compounds. It is well known that the oxidation of any compound involves multiple steps, and the use of the PTR-MS in these experiments showed, in real time, the evolution of the different ions as first and second-generation oxidation products. These detailed time series, in conjunction with observed yields, aid in understanding and elucidating likely reaction pathways and structures for the unidentified products.

[49] The PTR-MS is emerging as an important tool for the measurement of primary and secondary gas-phase compounds in field campaigns. Mass scans of ambient air will undoubtedly measure unidentified compounds, and concurrent or prior measurements of primary emissions at the given site will aid in narrowing the possible identities of the observed ions. Our results confirm that the product ions observed by [*Holzinger et al.*, 2005] are consistent with terpene photooxidation reactions. Many different oxidation products likely contribute to the ions observed in ambient air. Observations of unidentified products [*Holzinger et al.*, 2005] and knowledge of primary emissions [*Lee et al.*, 2005], together with the results reported here of the identified, tentatively identified, and unidentified oxidation products from primary terpene compounds, aid greatly in understanding the magnitude and significance of within-canopy oxidation. Because the detection of very reactive parent terpene emissions is difficult in ambient air, observations of the ions described in this study can serve as markers for within-canopy chemistry and reactivity, and thus of SOA production. Observations of these product ions are likely to be of significant interest to scientists conducting field measurements in atmospheric chemistry, biosphere-atmosphere exchange of volatile organic compounds, and secondary organic aerosol composition. Further experiments to identify the compounds contributing to the unidentified products are necessary and will be more useful to laboratory chemists and kineticists for the elucidation of more complete terpene oxidation mechanisms.

[50] **Acknowledgments.** This material is based upon work supported by the National Science Foundation under grants 0119510 and 0443448.

Additional support was provided by the California Air Resources Board (contract 00-732). A. Lee was supported by a Graduate Research Education Fellowship from the U.S. Department of Energy's Global Change Education Program. The Caltech Indoor Chamber Facility is supported by the U.S. Environmental Protection Agency Science to Achieve Results (STAR) Program grant RD-83107501-0, and the U.S. Department of Energy grant DE-FG02-05ER63983. The authors are grateful to R. Holzinger for help in transporting and installing the PTR-MS in the Caltech Indoor Chamber Facility. We also thank the two anonymous reviewers for their thorough review and helpful comments.

References

Arey, J., R. Atkinson, and S. M. Aschmann (1990), Product study of the gas-phase reactions of monoterpenes with the OH radical in the presence of NO_x, *J. Geophys. Res.*, *95*(D11), 18,539–18,546.

Aschmann, S. M., A. Reissell, R. Atkinson, and J. Arey (1998), Products of the gas phase reactions of the OH radical with alpha- and beta-pinene in the presence of NO, *J. Geophys. Res.*, *103*(D19), 25,553–25,561.

Aschmann, S. M., R. Atkinson, and J. Arey (2002), Products of reaction of OH radicals with alpha-pinene, *J. Geophys. Res.*, *107*(D14), 4191, doi:10.1029/2001JD001098.

Atkinson, R., and J. Arey (2003), Gas-phase tropospheric chemistry of biogenic volatile organic compounds: A review, *Atmos. Environ.*, *37*, S197–S219.

Atkinson, R., S. M. Aschmann, E. C. Tuazon, J. Arey, and B. Zielinska (1989), Formation of 3-methylfuran from the gas-phase reaction of OH radicals with isoprene and the rate-constant for its reaction with the OH radical, *Int. J. Chem. Kinet.*, *21*(7), 593–604.

Baker, J., J. Arey, and R. Atkinson (2005), Formation and reaction of hydroxycarbonyls from the reaction of OH radicals with 1,3-butadiene and isoprene, *Environ. Sci. Technol.*, *39*(11), 4091–4099.

Calogirou, A., D. Kotzias, and A. Kettrup (1997), Product analysis of the gas-phase reaction of b-caryophyllene with ozone, *Atmos. Environ.*, *31*(2), 283–285.

Ciccioli, P., et al. (1999), Emission of reactive terpene compounds from orange orchards and their removal by within-canopy processes, *J. Geophys. Res.*, *104*(D7), 8077–8094.

Claeys, M., et al. (2004), Formation of secondary organic aerosols through photooxidation of isoprene, *Science*, *303*(5661), 1173–1176.

Cocker, D. R., R. C. Flagan, and J. H. Seinfeld (2001), State-of-the-art chamber facility for studying atmospheric aerosol chemistry, *Environ. Sci. Technol.*, *35*(12), 2594–2601.

Day, D. A., P. J. Wooldridge, M. B. Dillon, J. A. Thornton, and R. C. Cohen (2002), A thermal dissociation laser-induced fluorescence instrument for in situ detection of NO_2, peroxy nitrates, alkyl nitrates and HNO3, *J. Geophys. Res.*, *107*(D6), 4046, doi:10.1029/2001JD000779.

Di Carlo, P., et al. (2004), Missing OH reactivity in a forest: Evidence for unknown reactive biogenic VOCs, *Science*, *304*(5671), 722–725.

Faloona, I., et al. (2001), Nighttime observations of anomalously high levels of hydroxyl radicals above a deciduous forest canopy, *J. Geophys. Res.*, *106*(D20), 24,315–24,333.

Farmer, D. K., P. J. Wooldridge, and R. C. Cohen (2005), Biosphere-atmosphere exchange of reactive nitrogen oxides over a midelevation Sierra Nevada forest, *Eos Trans. AGU*, *86*(52), Fall Meet. Suppl., Abstract A44B-01.

Goldstein, A. H., M. McKay, M. R. Kurpius, G. W. Schade, A. Lee, R. Holzinger, and R. A. Rasmussen (2004), Forest thinning experiment confirms ozone deposition to forest canopy is dominated by reaction with biogenic VOCs, *Geophys. Res. Lett.*, *31*, L22106, doi:10.1029/2004GL021259.

Griffin, R. J., D. R. Cocker, R. C. Flagan, and J. H. Seinfeld (1999), Organic aerosol formation from the oxidation of biogenic hydrocarbons, *J. Geophys. Res.*, *104*(D3), 3555–3567.

Grosjean, D., E. L. Williams, and J. H. Seinfeld (1992), Atmospheric oxidation of selected terpenes and related carbonyls - Gas-phase carbonyl products, *Environ. Sci. Technol.*, *26*(8), 1526–1533.

Guenther, A. B., et al. (1995), A global model of natural volatile organic compound emissions, *J. Geophys. Res.*, *100*, 8873–8892.

Hakola, H., J. Arey, S. M. Aschmann, and R. Atkinson (1994), Product formation from the gas-phase reactions of OH radicals and O_3 with a series of monoterpenes, *J. Atmos. Chem.*, *18*(1), 75–102.

Hatakeyama, S., K. Izumi, T. Fukuyama, H. Akimoto, and N. Washida (1991), Reactions of OH with alpha-pinene and beta-pinene in air: Estimate of global CO production from the atmospheric oxidation of terpenes, *J. Geophys. Res.*, *96*(D1), 947–958.

Hoffmann, T., J. R. Odum, F. Bowman, D. Collins, D. Klockow, R. C. Flagan, and J. H. Seinfeld (1997), Formation of organic aerosols from the oxidation of biogenic hydrocarbons, *J. Atmos. Chem.*, *26*(2), 189–222.

Holzinger, R., E. Sanhueza, R. von Kuhlmann, B. Kleiss, L. Donoso, and P. J. Crutzen (2002), Diurnal cycles and seasonal variation of isoprene and its oxidation products in the tropical savanna atmosphere, *Global Biogeochem. Cycles*, *16*(4), 1074, doi:10.1029/2001GB001421.

Holzinger, R., A. Lee, K. T. Paw U, and A. H. Goldstein (2005), Observations of oxidation products above a forest imply biogenic emissions of very reactive compounds, *Atmos. Chem. Phys.*, *5*, 1–9.

Jaoui, M., and R. M. Kamens (2001), Mass balance of gaseous and particulate products analysis from alpha-pinene/NO_x/air in the presence of natural sunlight, *J. Geophys. Res.*, *106*(D12), 12,541–12,558.

Jaoui, M., and R. M. Kamens (2003a), Gas and particle products distribution from the photooxidation of a-humulene in the presence of NO_x, natural atmospheric air and sunlight, *J. Atmos. Chem.*, *46*, 29–54.

Jaoui, M., and R. M. Kamens (2003b), Mass balance of gaseous and particulate products from beta-pinene/O_3/air in the absence of light and beta-pinene/NO_x/air in the presence of natural sunlight, *J. Atmos. Chem.*, *45*(2), 101–141.

Kavouras, I. G., N. Mihalopoulos, and E. G. Stephanou (1999), Formation and gas/particle partitioning of monoterpenes photo-oxidation products over forests, *Geophys. Res. Lett.*, *26*(1), 55–58.

Kesselmeier, J., and M. Staudt (1999), Biogenic volatile organic compounds (VOC): An overview on emission, physiology, and ecology, *J. Atmos. Chem.*, *33*, 23–88.

Keywood, M. D., V. Varutbangkul, R. Bahreini, R. C. Flagan, and J. H. Seinfeld (2004), Secondary organic aerosol formation from the ozonolysis of cycloalkenes and related compounds, *Environ. Sci. Technol.*, *38*(15), 4157–4164.

Kourtchev, I., T. Ruuskanen, W. Maenhaut, M. Kulmala, and M. Claeys (2005), Observation of 2-methyltetrols and related photo-oxidation products of isoprene in boreal forest aerosols from Hyytiala, Finland, *Atmos. Chem. Phys.*, *5*, 2761–2770.

Kroll, J. H., N. L. Ng, S. M. Murphy, R. C. Flagan, and J. H. Seinfeld (2005), Secondary organic aerosol formation from isoprene photooxidation under high-NO_x conditions, *Geophys. Res. Lett.*, *32*, L18808, doi:10.1029/2005GL023637.

Kroll, J. H., N. L. Ng, S. M. Murphy, R. C. Flagan, and J. H. Seinfeld (2006), Secondary organic aerosol formation from isoprene photooxidation, *Environ. Sci. Technol.*, *40*, 1869–1877.

Kurpius, M. R., and A. H. Goldstein (2003), Gas-phase chemistry dominates O_3 loss to a forest, implying a source of aerosols and hydroxyl radicals to the atmosphere, *Geophys. Res. Lett.*, *30*(7), 1371, doi:10.1029/2002GL016785.

Kwok, E. S. C., R. Atkinson, and J. Arey (1995), Observation of hydroxycarbonyls from the OH radical-initiated reaction of isoprene, *Environ. Sci. Technol.*, *29*(9), 2467–2469.

Lamanna, M. S., and A. H. Goldstein (1999), In situ measurements of C_2–C_{10} volatile organic compounds above a Sierra Nevada ponderosa pine plantation, *J. Geophys. Res.*, *104*(D17), 21,247–21,262.

Larsen, B. R., D. Di Bella, M. Glasius, R. Winterhalter, N. R. Jensen, and J. Hjorth (2001), Gas-phase OH oxidation of monoterpenes: Gaseous and particulate products, *J. Atmos. Chem.*, *38*(3), 231–276.

Lee, A., G. W. Schade, R. Holzinger, and A. H. Goldstein (2005), A comparison of new measurements of total monoterpene flux with improved measurements of speciated monoterpene flux, *Atmos. Chem. Phys.*, *5*, 505–513.

Lee, A., A. H. Goldstein, M. D. Keywood, S. Gao, V. Varutbangkul, R. Bahreini, N. L. Ng, R. C. Flagan, and J. H. Seinfeld (2006), Gas-phase products and secondary aerosol yields from the ozonolysis of ten different terpenes, *J. Geophys. Res.*, *111*, D07302, doi:10.1029/2005JD006437.

Librando, V., and G. Tringali (2005), Atmospheric fate of OH initiated oxidation of terpenes: Reaction mechanism of alpha-pinene degradation and secondary organic aerosol formation, *J. Environ. Manage.*, *75*(3), 275–282.

Lindinger, W., A. Hansel, and A. Jordan (1998), Proton-transfer-reaction mass spectrometry (PTR-MS): On-line monitoring of volatile organic compounds at pptv levels, *Chem. Soc. Rev.*, *27*(5), 347–354.

Matsunaga, S. N., C. Wiedinmyer, A. B. Guenther, J. J. Orlando, T. Karl, D. W. Toohey, J. P. Greenberg, and Y. Kajii (2005), Isoprene oxidation products are a significant atmospheric aerosol component, *Atmos. Chem. Phys. Discuss.*, *5*, 11,146–11,156.

Miyoshi, A., S. Hatakeyama, and N. Washida (1994), OH radical-initiated photooxidation of isoprene: An estimate of global CO production, *J. Geophys. Res.*, *99*(D9), 18,779–18,787.

Ng, N. L., J. H. Kroll, M. D. Keywood, R. Bahreini, V. Varutbangkul, R. C. Flagan, J. H. Seinfeld, A. Lee, and A. H. Goldstein (2006), Contribution of first- versus second-generation products to secondary organic aerosols formed in the oxidation of biogenic hydrocarbons, *Environ. Sci. Technol.*, *40*, 2283–2297.

Noziere, B., and I. Barnes (1998), Evidence for formation of a PAN analogue of pinonic structure and investigation of its thermal stability, *J. Geophys. Res.*, *103*(D19), 25,587–25,597.

Noziere, B., M. Spittler, L. Ruppert, I. Barnes, K. H. Becker, M. Pons, and K. Wirtz (1999), Kinetics of the reactions of pinonaldehyde with OH radicals and with Cl atoms, *Int. J. Chem. Kinet.*, *31*(4), 291–301.

Orlando, J. J., B. Noziere, G. S. Tyndall, G. E. Orzechowska, S. E. Paulson, and Y. Rudich (2000), Product studies of the OH- and ozone-initiated oxidation of some monoterpenes, *J. Geophys. Res.*, *105*(D9), 11,561–11,572.

Pandis, S. N., S. E. Paulson, J. H. Seinfeld, and R. C. Flagan (1991), Aerosol formation in the photooxidation of isoprene and beta-pinene, *Atmos. Environ., Part A*, *25*(5–6), 997–1008.

Paulson, S. E., R. C. Flagan, and J. H. Seinfeld (1992), Atmospheric photooxidation of isoprene. 1. The hydroxyl radical and ground-state atomic oxygen reactions, *Int. J. Chem. Kinet.*, *24*(1), 79–101.

Peeters, J., L. Vereecken, and G. Fantechi (2001), The detailed mechanism of the OH-initiated atmospheric oxidation of alpha-pinene: A theoretical study, *Phys. Chem. Chem. Phys.*, *3*(24), 5489–5504.

Reissell, A., C. Harry, S. M. Aschmann, R. Atkinson, and J. Arey (1999), Formation of acetone from the OH radical- and O_3-initiated reactions of a series of monoterpenes, *J. Geophys. Res.*, *104*(D11), 13,869–13,879.

Reissell, A., S. M. Aschmann, R. Atkinson, and J. Arey (2002), Products of the OH radical- and O_3-initiated reactions of myrcene and ocimene, *J. Geophys. Res.*, *107*(D12), 4138, doi:10.1029/2001JD001234.

Schade, G. W., and A. H. Goldstein (2003), Increase of monoterpene emissions from a pine plantation as a result of mechanical disturbances, *Geophys. Res. Lett.*, *30*(7), 1380, doi:10.1029/2002GL016138.

Shu, Y. G., and R. Atkinson (1994), Rate constants for the gas-phase reactions of O_3 with a series of terpenes and OH radical formation from the O_3 reactions with sesquiterpenes at 296 ± 2-K, *Int. J. Chem. Kinet.*, *26*(12), 1193–1205.

Shu, Y. H., E. S. C. Kwok, E. C. Tuazon, R. Atkinson, and J. Arey (1997), Products of the gas-phase reactions of linalool with OH radicals, NO_3 radicals, and O_3, *Environ. Sci. Technol.*, *31*(3), 896–904.

Song, C., N. Kwangsam, and D. R. Cocker (2005), Impact of hydrocarbon to NO_x ratio on secondary organic aerosol formation, *Environ. Sci. Technol.*, *39*, 3143–3149.

Sprengnether, M., K. L. Demerjian, N. M. Donahue, and J. G. Anderson (2002), Product analysis of the OH oxidation of isoprene and 1,3-butadiene in the presence of NO, *J. Geophys. Res.*, *107*(D15), 4268, doi:10.1029/2001JD000716.

Tuazon, E. C., and R. Atkinson (1990), A product study of the gas-phase reaction of isoprene with the OH radical in the presence of NO_x, *Int. J. Chem. Kinet.*, *22*(12), 1221–1236.

Vereecken, L., and J. Peeters (2004), Nontraditional (per)oxy ring-closure paths in the atmospheric oxidation of isoprene and monoterpenes, *J. Phys. Chem. A*, *108*(24), 5197–5204.

Vinckier, C., F. Compernolle, A. M. Saleh, N. Van Hoof, and I. Van Hees (1998), Product yields of the alpha-pinene reaction with hydroxyl radicals and the implication on the global emission of trace compounds in the atmosphere, *Fresenius Environ. Bull.*, *7*(5–6), 361–368.

Warneke, C., et al. (2001), Isoprene and its oxidation products methyl vinyl ketone, methacrolein, and isoprene related peroxides measured online over the tropical rain forest of Surinam in March 1998, *J. Atmos. Chem.*, *38*, 167–185.

Wisthaler, A., N. R. Jensen, R. Winterhalter, W. Lindinger, and J. Hjorth (2001), Measurements of acetone and other gas phase product yields from the OH-initiated oxidation of terpenes by proton-transfer-reaction mass spectrometry (PTR-MS), *Atmos. Environ.*, *35*(35), 6181–6191.

Yu, J. Z., R. J. Griffin, D. R. Cocker, R. C. Flagan, J. H. Seinfeld, and P. Blanchard (1999), Observation of gaseous and particulate products of monoterpene oxidation in forest atmospheres, *Geophys. Res. Lett.*, *26*(8), 1145–1148.

Zhao, J., R. Zhang, E. C. Fortner, and S. W. North (2004), Quantification of hydroxycarbonyls from OH-isoprene reactions, *J. Am. Chem. Soc.*, *126*, 2686–2687.

R. C. Flagan, J. H. Kroll, N. L. Ng, J. H. Seinfeld, and V. Varutbangkul, Department of Environmental Science and Engineering and Department of Chemical Engineering, California Institute of Technology, Pasadena, CA 91125, USA.

A. H. Goldstein and A. Lee, Department of Environmental Science, Policy, and Management, University of California, Berkeley, Berkeley, CA 94720-3114, USA. (ahg@nature.berkeley.edu)